



Title	A Genomic Region Transcribed Into a Long Noncoding RNA Interacts With the Prss42/Tessp-2 Promoter in Spermatocytes During Mouse Spermatogenesis, and Its Flanking Sequences Can Function as Enhancers
Author(s)	Yoneda, Ryoma; Satoh, Yui; Yoshida, Ikuya; Kawamura, Shohei; Kotani, Tomoya; Kimura, Atsushi P.
Citation	Molecular reproduction and development, 83(6), 541-557 https://doi.org/10.1002/mrd.22650
Issue Date	2016-06
Doc URL	http://hdl.handle.net/2115/65841
Rights	This is the peer reviewed version of the following article: Yoneda, R., Satoh, Y., Yoshida, I., Kawamura, S., Kotani, T. and Kimura, A. P. (2016), A genomic region transcribed into a long noncoding RNA interacts with the Prss42/Tessp-2 promoter in spermatocytes during mouse spermatogenesis, and its flanking sequences can function as enhancers. Mol. Reprod. Dev., 83: 541–557, which has been published in final form at doi:10.1002/mrd.22650. This article may be used for non-commercial purposes in accordance with Wiley Terms and Conditions for Self-Archiving
Type	article (author version)
File Information	A Genomic Region Transcribed.pdf



[Instructions for use](#)

A Genomic Region Transcribed into a Long Noncoding RNA Interacts with the *Prss42/Tessp-2* Promoter in Spermatocytes during Mouse Spermatogenesis and its Flanking Sequences Can Function as Enhancers

Ryoma Yoneda,¹ Yui Satoh,¹ Ikuya Yoshida,^{1,2} Shohei Kawamura,¹ Tomoya Kotani,^{1,2} and Atsushi P. Kimura^{1,2*}

¹ Graduate School of Life Science, Hokkaido University, Sapporo 060-0810, Japan

² Department of Biological Sciences, Faculty of Science, Hokkaido University, Sapporo 060-0810, Japan

*Corresponding author: Department of Biological Sciences, Faculty of Science, Hokkaido University, Sapporo 060-0810, Japan. E-mail: akimura@sci.hokudai.ac.jp

Present address of Ryoma Yoneda is Research Center for Genomic Medicine, Saitama Medical University, Hidaka 350-1241, Japan

Ryoma Yoneda and Yui Satoh contributed equally to this work.

Running title: *Tessp-2* enhancers adjacent to a lncRNA

Keywords: Prss/Tessp, enhancer, long noncoding RNA, male meiosis, spermatocyte, chromosome conformation capture

Abbreviations: 3C, chromosome conformation capture; BAC, bacterial artificial chromosome; cDNA, complementary DNA; CIAA, chloroform isoamylalcohol; DIG, digoxigenin; EC, embryonal

carcinoma; HS, hypersensitive site; lncRNA, long noncoding RNA; PBS, phosphate buffered saline; PCR, polymerase chain reaction; Prss, protease serine; RACE, rapid amplification of complimentary DNA ends; RT-PCR, reverse transcription-polymerase chain reaction; SD, standard deviation; Tessp, testis-specific serine protease; TSA, tyramide signal amplification; TSS, transcriptional start site; TTS, transcriptional termination site

Grant Sponsor: Grant-in-aid for Young Scientists 21770068, Grant-in-aid for Scientific Research 15H04317, and Grant-in-aid for JSPS Fellows 23-6804 from Japan Society for the Promotion of Science.

SUMMARY

Spermatogenesis is precisely regulated by many meiotic stage-specific genes, but their regulatory mechanisms are not fully understood. The *Prss/Tessp* gene cluster is located on the mouse chromosome 9F2-F3, and the three genes, *Prss42/Tessp-2*, *Prss43/Tessp-3*, and *Prss44/Tessp-4* on the cluster, are specifically activated in pachytene spermatocytes during meiosis. To elucidate a mechanism of their activation, we searched for DNase I hypersensitive sites (HSs) and long noncoding RNAs (lncRNAs) at the *Prss/Tessp* locus. We found eight DNase I HSs, three of which were testicular germ cell-specific at or close to the *Prss42/Tessp-2* promoter, and a testis-specific lncRNA, *lncRNA-HSVIII*, which was transcribed from 3' to the *Prss42/Tessp-2* gene. By in situ hybridization, *lncRNA-HSVIII* was localized in nuclei of most pachytene spermatocytes and in cytosols of pachytene spermatocytes at stage X and spermatids. Chromosome conformation capture assay showed that the chromatin at *lncRNA-HSVIII* specifically interacted with the *Prss42/Tessp-2* promoter in primary and secondary spermatocytes. By reporter gene assay, a 5.8-kb genome sequence, encompassing the entire *lncRNA-HSVIII* sequence and its flanking regions, significantly increased *Prss42/Tessp-2* promoter activity, but transfection of this construct did not change the *lncRNA-HSVIII* expression, which indicated that the increased promoter activity was likely to be dependent on enhancer activity. Indeed, we found that both upstream and downstream regions of the *lncRNA-HSVIII* sequence significantly increased *Prss42/Tessp-2* promoter activity. Our data indicate the direct interaction of a genomic region at *lncRNA-HSVIII* with the *Prss42/Tessp-2* promoter in spermatocytes and suggest that adjacent sequences to the lncRNA function as enhancers for the *Prss42/Tessp-2* gene.

INTRODUCTION

Spermatogenesis is a process to generate spermatozoa, but its mechanistic details, e.g., how genes are specifically activated at particular stages during meiosis, especially in primary spermatocytes, remains to be elucidated (Grimes, 2004; Shima et al., 2004; Wang et al., 2005; Johnston et al., 2008; Goldberg et al., 2010; Ou et al., 2010). We have studied three paralogous mouse genes, *Prss42/Tessp-2*, *Prss43/Tessp-3*, and *Prss44/Tessp-4*, which constitute a gene cluster on the mouse chromosome 9F2-F3 and are activated in primary spermatocytes at the late pachytene stage (Yoneda et al., 2013). The three genes encode serine proteases that are considered to play crucial roles in the progression of meiosis at different stages, together with another homologous gene, *Prss41/Tessp-1* (Yoneda and Kimura, 2013; Yoneda et al., 2013). Functional significance and spermatocyte-specific expression of the *Prss/Tessp* genes indicate that this gene cluster can serve as an excellent model for studying the mechanisms of gene activation during meiosis.

Classically, germ cell-specific genes were considered to be controlled solely by their proximal promoters, because many studies reported that minimum promoters were sufficient to activate such genes by generating transgenic mice (Reddi et al., 2007; Kehoe et al., 2008). In addition, general transcription factors that are exclusively expressed in testicular germ cells are known to play important roles in gene activation during meiosis (DeJong, 2006; Goodrich and Tjian, 2010). However, it is becoming clear that distal enhancer elements are required for the germ cell-specific gene activation. For example, the enhancer located between -4.8 kb and -1.3 kb of the transcriptional start site (TSS) was necessary for full activation of the mouse *Ccna1* gene (Lele and Wolgemuth, 2004), and we recently found an enhancer for the spermatocyte-specific mouse *Tcam1* gene (Kurihara et al., 2014). Therefore, the mechanisms of gene activation during male meiosis should be much more complicated.

In general, the regulation of chromatin structure is key to gene activation, and DNase I hypersensitivity reflects the chromatin state. DNase I hypersensitive site (HS) is a genome region with loose chromatin which is often marked with epigenetic modifications leading to the formation of

active chromatin (Jenuwein and Allis, 2001; Alabert and Groth, 2012; Mercer et al., 2013) and associated with promoters and enhancers (Cockerill, 2011; Iwafuchi-Doi and Zaret, 2014). Enhancers increase the transcription rate of their target genes by physically interacting with promoters, as revealed by the innovative chromosome conformation capture (3C) assay (Dekker et al., 2002; Tolhuis et al., 2002). Recently, some enhancers were found to be controlled by long noncoding RNAs (lncRNAs) (Zaratiegui et al., 2007; Umlauf et al., 2008; Ponting et al., 2009; Wilusz et al., 2009; Wang and Chang, 2011), which were extensively transcribed from mammalian genome in many tissues including the mouse testis (Bao et al., 2013; Sun et al., 2013; Liang et al., 2014; Necsulea et al., 2014). In those cases, lncRNAs were necessary for the dynamic chromatin rearrangement allowing enhancers to contact promoter regions (Sanyal et al., 2012; Lai et al., 2013; Li et al., 2013). However, whereas regulatory mechanisms of various tissue-specific genes have been identified (Arvey et al., 2012; Natarajan et al., 2012; Todeschini et al., 2014), it is unclear how DNase I HSs and lncRNAs are related to the specific gene activation in the testis during meiosis.

In this study, we attempted to reveal the mechanism of activation of the *Prss/Tessp* gene cluster. We found eight DNase I HSs at the locus and a testis-specific lncRNA, *lncRNA-HSVIII*, which was transcribed from 3' to the *Prss42/Tessp-2* gene. Interestingly, in spermatocytes, the chromatin at *lncRNA-HSVIII* interacted with the *Prss42/Tessp-2* promoter, in which germ cell-specific DNase I HSs were present. However, the *lncRNA-HSVIII* transcription was unlikely to be related to the *Prss42/Tessp-2* gene regulation, and instead, adjacent sequences to the lncRNA possessed enhancer activity for the *Prss42/Tessp-2* promoter. The study provides a model for a novel mechanism of gene activation during male meiosis.

RESULTS

DNase I HS Mapping at the Mouse *Prss/Tessp* Locus

To identify cis-regulatory sequences for *Prss/Tessp* genes, we performed DNase I HS mapping on the *Prss/Tessp* genes and their adjacent regions in testicular germ cells and liver cells. The germ cell fraction was prepared as previously described (Yoneda et al., 2013), and we confirmed that more than 70% of cells in the fraction were germ cells based on the marker gene expression in this study. The liver was used as a tissue which did not express any of the cluster genes. The nuclei from germ cells and liver cells were treated with DNase I, and DNAs were purified, digested with restriction enzymes, and subjected to Southern blot analysis.

We first examined two restriction fragments, digested with *HindIII* and *BamHI*, which covered a 38-kb region encompassing the *Prss42/Tessp-2* gene (Fig. 1A). By *HindIII* digestion, we detected a mother band at the position of 20 kb as expected and three additional bands: two at 11.9 kb and 1.2 kb in both native germ cells and liver cells, and one at 9.9 kb only in the liver (Fig. 1B). These DNase I HSs corresponded to 13.3 kb, 11.3 kb, and 2.7 kb upstream of the *Prss42/Tessp-2* gene, and we named them HSI, HSII, and HSIII (Fig. 1A and B). The band corresponding to HSI was observed before DNase I treatment in the liver, possibly due to endogenous DNase activity. By *BamHI* digestion, we observed a mother band at 22 kb as expected and four additional bands: two at 11.1 kb and 4.9 kb in both tissues, one at 6.7 kb only in the liver, and the other one at 3.9 kb only in native germ cells, although the signal intensity was different between the two cell types (Fig. 1C). These DNase I HSs corresponded to the promoter, gene body, and 3' flanking region of the *Prss42/Tessp-2* gene.

The presence of DNase I HSs at the *Prss42/Tessp-2* promoter was consistent with the active transcription of this gene in native germ cells, but we also detected a band corresponding to this promoter in liver cells by *BamHI* digestion (Fig. 1C, arrowhead). Thus, we performed fine mapping at this region by digestion with *EcoRI*. The Southern blot analysis resulted in the detection of a mother band at 3.6 kb as expected in both cells. In germ cells, three additional bands were observed at 2.4 kb, 1.5 kb, and 1.2 kb, whereas no clear band was detected in the liver (Fig. 1D). The lack of DNase I HS in the liver was not due to insufficient DNase I treatment, because the gel image after ethidium bromide staining indicated a similar extent of digestion to germ cell nuclei (Fig. S1). The DNase I HSs

in the *EcoRI* fragment were considered to be germ cell-specific. As a result of mapping these DNase I HSs at the locus, the 2.4-kb band corresponded to the signal at 3.9 kb by *BamHI* digestion, and the other two bands were presumed to be detected as one *BamHI* fragment at 4.9 kb. We named these DNase I HSs HSIV, HSV, and HSVI (Fig. 1C and D), and then, the DNase I HSs located downstream to them were named HSVII and HSVIII (Fig. 1C).

Consequently, we found eight DNase I HSs at the *Prss42/Tessp-2* locus: two of them (HSII and HSVII) were liver-specific, and three at or close to the *Prss42/Tessp-2* promoter (HSIV, HSV, and HSVI) were present only in testicular germ cells (Fig. 1A).

Characterization of *lncRNA-HSVIII* Transcribed from 3' to the *Prss42/Tessp-2* gene

We next assessed noncoding transcription at the *Prss/Tessp* locus because lncRNAs are important for regulation of various genes (Rinn and Chang, 2012) and there are many lncRNAs expressed in the testis (Bao et al., 2013; Sun et al., 2013; Liang et al., 2014). Based on transcriptomic data (accession numbers: SRX135150, SRX135160, and SRX135162), we found that several intergenic regions were specifically transcribed in the testis at the *Prss/Tessp* locus. As a result of reverse transcription-polymerase chain reaction (RT-PCR) analyses, we identified a novel lncRNA transcribed from the downstream region of the *Prss42/Tessp-2* gene and named it *lncRNA-HSVIII* (Fig. 2A). This lncRNA was specifically detected by RT-PCR in samples of total RNA from whole testis (Fig. 2B). We then examined which types of cells expressed *lncRNA-HSVIII* by fractionating testicular cells. We prepared germ, Sertoli, and Sertoli/Leydig cell fractions, and the expression of marker genes indicated that the fractionation was successful (Fig. S2). By RT-PCR, we detected the transcript in germ and Sertoli/Leydig cell fractions but not in Sertoli cell fraction (Fig. 2C). The Sertoli cell fraction did not contain any other cell types (Fig. S2) and showed no signal for *lncRNA-HSVIII* (Fig. 2C), so the signal in the Sertoli/Leydig cell fraction was likely to originate from Leydig cells. Therefore, *lncRNA-HSVIII* was presumed to be expressed in germ cells and Leydig cells, and the stronger signal in the germ cell fraction might represent its main role in meiosis. We also examined subcellular localization of this

lncRNA by RT-PCR with nuclear and cytosolic RNAs of germ cells, and found that it was localized predominantly in the nucleus but was also present in the cytosol (Fig. 2D).

These results suggested that *lncRNA-HSVIII* was involved in the germ cell-specific regulation of *Prss/Tessp* genes. Thus, we decided to determine the full-length sequence of *lncRNA-HSVIII* by rapid amplification of cDNA ends (RACE) analyses. Using a 5'RACE procedure, in 20 subclones, we detected one TSS of *lncRNA-HSVIII*. On the other hands, 3'RACE resulted in the identification of three transcriptional termination sites (TTSs) by sequencing 10 subclones. Interestingly, there were the repeat of GAAAA sequence in the 3' region, and the subclones had different numbers of this sequence. Seven subclones had a final adenine of the 7th GAAAA sequence as TTS, and the 3rd and 10th GAAAA was TTS in one and two subclones, respectively. Thus, we determined the 7th GAAAA as the 3' end of *lncRNA-HSVIII*. Consequently, the full-length of *lncRNA-HSVIII* was determined to be 2665 nucleotides long (Fig. 2A) and it had a poly(A) tail. The nucleotide sequence was deposited to DDBJ/EMBL/GenBank databases under the accession number LC060751.

To further analyze the expression pattern of *lncRNA-HSVIII*, we performed in situ hybridization with the highly sensitive tyramide signal amplification (TSA) system using adult testes. We detected many signals as red dots with the antisense probe of *lncRNA-HSVIII*, whereas few dots were observed with the sense probe (Fig. 3A and B). Consistent with the RT-PCR result of fractionated testicular cells (Fig. 2C), positive signals were present not only in germ cells but also in nuclei and cytosols of Leydig cells (Fig. 3C, arrows). In seminiferous tubules, positive red signals were observed at all seminiferous epithelial stages. At stage V, a few signals were observed in nuclei of pachytene spermatocytes and in cytosols of spermatids (Fig. 3D). While the signals in spermatids remained, those in nuclei of pachytene spermatocytes increased at stage VIII (Fig. 3E). At stage X, more red dots were observed in nuclei of some pachytene spermatocytes and in cytosols of the others (Fig. 3F). These results indicated that the *lncRNA-HSVIII* transcription was activated in early pachytene spermatocytes and enhanced at late pachytene stages, during which the transcripts were localized to nuclei, and at the end of the pachytene spermatocyte stage, *lncRNA-HSVIII* changed its localization to cytosols and the cytosolic

RNAs were retained in spermatids.

Spermatocyte-Specific Interaction of the Chromatin at *lncRNA-HSVIII* with the *Prss42/Tessp-2*

Promoter

In pachytene spermatocytes, it was possible that *lncRNA-HSVIII* transcription contributed to activation of the *Prss/Tessp* cluster genes. In general, cis-acting lncRNAs require the interaction of genomic regions transcribed into them with their target promoters or mediate the interaction of enhancers with promoters for gene activation (Zaratiegui et al., 2007; Umlauf et al., 2008; Ponting et al., 2009; Wilusz et al., 2009; Wang and Chang, 2011;). Thus, we investigated whether the chromatin at *lncRNA-HSVIII* interacted with any of *Prss/Tessp* promoters by 3C assay. Since many lncRNAs interacted with their target promoters via their 3' regions (Lai et al., 2013; Xiang et al., 2014), we designed an anchor primer at 3' of the *lncRNA-HSVIII* region and examined the interaction with HSI, HSIV, and promoters of the three *Prss/Tessp* genes (Fig. 4A). The interaction frequency was normalized to that of the control in which a bacterial artificial chromosome (BAC) clone encompassing the *Prss/Tessp* cluster was digested and ligated. The value was further normalized to the frequency at the *Ercc3* locus which is thought to show positive interaction at similar levels in many tissues (Palstra et al., 2003). Relative interaction frequency at the *Ercc3* locus was set to 1.0.

We first performed 3C assay using testicular germ cells and liver cells. While we did not detect significant levels of interaction with any regions in liver cells, HSIV and the *Prss42/Tessp-2* promoter were found to interact with the *lncRNA-HSVIII* region in germ cells (Fig. 4B). The interaction frequency with HSIV in germ cells was significantly higher than that in the liver and was comparable to the level at the *Ercc3* locus. The frequency with the *Prss42/Tessp-2* promoter was also significantly higher in germ cells than in the liver, and the level was about one third of that at the *Ercc3* locus. When we performed this experiment without DNA ligase, no significant signals were detected by PCR (data not shown).

We next fractionated germ cells by a cell sorter into four meiotic stages; spermatogonia, primary

spermatocytes, secondary spermatocytes, and spermatids/spermatozoa, as previously described (Yoneda et al., 2013). By performing 3C assay with the fractionated cells, we detected significant levels of interaction in spermatocytes but not in spermatogonia and spermatids/spermatozoa (Fig. 4C). In primary spermatocytes, HSIV and the *Prss42/Tessp-2* promoter interacted with the *lncRNA-HSVIII* region at significantly higher levels than in spermatogonia, and the interaction frequency with HSIV increased in secondary spermatocytes (Fig. 4C). The interaction disappeared in the fraction of spermatids and spermatozoa (Fig. 4C). Taken together with our previous findings that *Prss42/Tessp-2* was activated in primary spermatocytes and its transcription was maintained in secondary spermatocytes but declined in spermatids/spermatozoa (Yoneda et al., 2013), these results suggested that the interaction of the chromatin at *lncRNA-HSVIII* with upstream regions of the *Prss42/Tessp-2* promoter was necessary for the spermatocyte-specific *Prss42/tessp-2* activation. We assumed that either *lncRNA-HSVIII* transcription or enhancer elements within or close to it were involved in the *Prss42/Tessp-2* gene activation.

Enhancer Activity in the Region Encompassing *lncRNA-HSVIII*

To determine whether *lncRNA-HSVIII* transcription was related to *Prss42/Tessp-2* activation or the genomic sequence encompassing it functioned as an enhancer for *Prss42/Tessp-2*, we prepared a reporter construct containing a 5.8-kb *EcoRI* fragment fused with the luciferase gene driven by the *Prss42/Tessp-2* promoter (Fig. 5). This 5.8-kb fragment encompassed the entire sequence of *lncRNA-HSVIII* as well as its 1.9-kb promoter and 1.2-kb 3' sequence (Fig. 5A). For comparison, we also prepared a construct without the 5.8-kb fragment and that with a 6.7-kb λ *HindIII* fragment (Fig. 5B and C). In luciferase reporter assays, we used two established mouse cell lines, an embryonal carcinoma (EC) cell line, P19TG1, and a hepatic tumor line, Hepa1-6, because both endogenously expressed *Prss42/Tessp-2* mRNA (data not shown).

We introduced the constructs into P19TG1 and Hepa1-6 cells and measured luciferase activity two days later. The activity was significantly higher in the construct with the 5.8-kb fragment than

those without it and with the λ DNA in both cells (Fig. 5B and C). To examine whether this enhancement of *Prss42/Tessp-2* promoter activity was associated with *lncRNA-HSVIII* transcription, we measured the *lncRNA-HSVIII* level in P19TG1 and Hepa1-6 cells transfected with the construct with or without the 5.8-kb fragment. By quantitative RT-PCR, levels of the *lncRNA-HSVIII* transcript were not significantly different between the two constructs in P19TG1 cells (Fig. 6). In Hepa1-6 cells, we could not detect any levels of the *lncRNA-HSVIII* transcript with either construct (data not shown). Thus, *lncRNA-HSVIII* was not transcribed from the transgene, which strongly suggested that the 5.8-kb sequence increased *Prss42/Tessp-2* promoter activity by functioning as an enhancer element in P19TG1 and Hepa1-6 cells.

We finally assessed which region in the 5.8-kb sequence possessed enhancer activity by separating it into three regions: 2.3-kb upstream region, 2.7-kb *lncRNA-HSVIII* sequence, and 1.5-kb downstream region (Fig. 5A). As a result of transfection and luciferase activity assay, the *lncRNA-HSVIII* sequence itself showed no enhancer activity in either P19TG1 cells or Hepa1-6 cells (Fig. 7A). In contrast, both upstream and downstream sequences of *lncRNA-HSVIII* significantly increased *Prss42/Tessp-2* promoter activity in both cells (Fig. 7B). This indicated that the flanking sequences to *lncRNA-HSVIII* possessed enhancer activity for the *Prss42/Tessp-2* gene, which suggests that genomic regions adjacent to *lncRNA-HSVIII* function as enhancers for the *Prss42/Tessp-2* gene in spermatocytes.

DISCUSSION

Many studies reported that testicular germ cell-specific genes were controlled exclusively by their proximal promoters (Reddi et al., 2007). However, even if a promoter was sufficient to germ cell-specific gene activation, the transgene was often silenced or the expression level varied between transgenic lines (Robinson et al., 1989; Zambrowicz et al., 1993; S. Li et al., 1998; Reddi et al., 1999;

Han et al., 2004). This indicates that other elements such as insulators and distal enhancers are required for germ cell-specific gene regulation. Actually, the presence of enhancers functioning during male meiosis was reported for some genes (Lele and Wolgemuth, 2004; Kurihara et al., 2014). Our current data provide another evidence of the potential presence of enhancers for a spermatocyte-specific gene and highlight the complicated mechanism for gene activation during meiosis.

In this study, we first searched for DNase I HSs to identify cis-regulatory sequences that were involved in the activation of *Prss/Tessp* genes. Although we found eight DNase I HSs, three germ cell-specific ones were all positioned in the *Prss42/Tessp-2* promoter or close to it (Fig. 1). This might suggest that the *Prss42/Tessp-2* promoter possessed major activity for the spermatocyte-specific gene activation, as exemplified by the *Pgk2* and *Prm1* promoter containing DNase I HSs and being mostly sufficient for their meiotic stage-specific activation (Peschon et al., 1987, 1989; Robinson et al., 1989; Kumari et al., 1996; Kramer et al., 1998; Martins and Krawetz, 2007). However, ubiquitously distributed DNase I HSs could possibly function for tissue-specific gene expression, and enhancers were not necessarily associated with DNase I hypersensitivity. Therefore, while the *Prss42/Tessp-2* promoter was obviously important for its spermatocyte-specific expression, we thought that there were distal cis-regulatory elements of this gene. In fact, we found potential enhancer sequences at 3' to the *Prss42/Tessp-2* gene and focused on their characterization.

The presence of potential enhancers for *Prss42/Tessp-2* but not for the other two cluster genes is remarkable given that *Prss42/Tessp-2* mRNA is expressed at the highest level in three cluster genes (Yoneda et al., 2013). Although it is unclear whether *Prss44/Tessp-4* and *Prss43/Tessp-3* genes are mostly regulated by their promoters, the chromatin interaction of potential enhancer elements with the *Prss42/Tessp-2* promoter but not with the other *Prss/Tessp* promoters suggests different regulatory mechanisms for the cluster genes. While the *Prss42/Tessp-2* gene may be regulated by a complicated mechanism involving several regulatory elements, proximal promoters may be sufficient for activating the other two genes.

Long range chromatin interaction is very important in the regulation of many genes in various tissues (Sipos and Gyurkovics, 2005; Bartkuhn and Renkawitz, 2008; Ghirlando et al., 2012), but there have been no such reports in testicular germ cells. Here we provide such an example, but more importantly, we revealed dynamic changes of the chromatin conformation during meiosis. Our data clearly indicated the stage-specific interaction of the *lncRNA-HSVIII* region with the *Prss42/Tessp-2* promoter as follows: in spermatogonia, the chromatin at *lncRNA-HSVIII* did not interact with the *Prss42/Tessp-2* promoter, then these two sites physically interacted in primary and secondary spermatocytes, but their interaction disappeared in spermatids (Fig. 4). The stages at which this long range chromatin interaction was observed coincided with those when *Prss42/Tessp-2* mRNA was expressed (Yoneda et al., 2013). This strongly suggests that the dynamic chromatin rearrangement is critical to *Prss42/Tessp-2* activation.

For *Prss42/Tessp-2* activation, we tested two possibilities: enhancer activity of genomic sequences encompassing *lncRNA-HSVIII* and the activation by *lncRNA-HSVIII* transcription. Although they were not mutually exclusive, we attempted to distinguish between these possibilities by generating a reporter construct, in which the luciferase gene driven by the *Prss42/Tessp-2* promoter was connected to a 5.8-kb fragment encompassing the entire *lncRNA-HSVIII* and its flanking sequences. As a result, this sequence showed enhancer activity in two cell lines expressing the *Prss42/Tessp-2* gene, while *lncRNA-HSVIII* was not transcribed from the transgene (Figs. 5 and 6). This indicated that the *Prss42/Tessp-2* promoter seemed to be regulated by an enhancer, but we further performed two additional experiments to exclude the possibility of lncRNA-mediated gene regulation. First, we overexpressed *lncRNA-HSVIII* in three cell lines, Hepa1-6, P19TG1, and GC-2spd(ts) cells, but mRNA levels of *Prss/Tessp* cluster genes were not changed in any cells (data not shown). GC-2spd(ts) cells were established from mouse primary spermatocytes (Hofmann et al., 1994). Second, by reporter gene assay, overexpression of *lncRNA-HSVIII* did not increase *Prss42/Tessp-2* promoter activity in Hepa1-6 cells (data not shown). Taken together with the observation that *lncRNA-HSVIII* was not necessarily localized in nuclei of the late stage of pachytene spermatocytes that were actively

transcribing *Prss/Tessp* genes (Fig. 3), we conclude that *lncRNA-HSVIII* does not contribute to transcriptional activation of the cluster.

Even if *lncRNA-HSVIII* is not related to the regulation of *Prss/Tessp* cluster genes, it probably contributes to the regulation of meiosis, and interestingly, the function of this lncRNA should be different between meiotic stages. In most pachytene spermatocytes, *lncRNA-HSVIII* was localized to nuclei, and its expression level dramatically increased at late pachytene stages (Fig. 3). Nuclear lncRNAs generally have one of the two functions: construction of nuclear structures such as paraspeckles and transcriptional activation or silencing (Chen and Carmichael, 2010). At present, we do not know how *lncRNA-HSVIII* functions in pachytene spermatocytes, but because we did not identify any specific nuclear structure associated with this lncRNA, it might control the transcription of spermatocyte-specific genes. In spermatids and some pachytene spermatocytes at stage X, *lncRNA-HSVIII* was localized in cytosols (Fig. 3F). Cytosolic lncRNAs reported so far are involved in the regulation of RNA stability and translation (Wu and Brewer, 2012; Atianand and Fitzgerald, 2014). Because many transcripts are under translational arrest in early stages of primary spermatocytes and their translation takes place at later stages (Morales et al., 1991; Langford et al., 1993; Schäfer et al., 1995; Yan et al., 2010), the cytosolic *lncRNA-HSVIII* may play a role in the translational control at this stage.

Instead of the contribution of *lncRNA-HSVIII*, we found that genomic sequences adjacent to it could function as enhancers for the *Prss42/Tessp-2* gene in EC cells (P19TG1) and hepatic tumor cells (Hepa1-6). Although these cells endogenously expressed *Prss42/Tessp-2* mRNA, it is a critical question whether the adjacent sequences to *lncRNA-HSVIII* really function as enhancers in native spermatocytes. In this context, it is notable that many testis-specific genes were activated in various tumor cells (Simpson et al., 2005), which suggests that activation mechanisms of testis specific-genes are partly common between in the testis and in the cell lines we used. Considering that similar enhancer activity was observed in two unrelated cell lines that expressed *Prss42/Tessp-2* mRNA (Figs. 5 and 7), our data supports that the flanking sequences to *lncRNA-HSVIII* really function as enhancers

for the *Prss42/Tessp-2* gene in the testis.

However, it is also true that cell lines do not completely resemble native tissues. Hepa1-6 cells were derived from mouse hepatoma (Darlington et al., 1980; Darlington, 1987) and have been widely used to study biological events in the liver as well as for other purposes. P19TG1 is an HPRT-deficient subline of P19 EC cell line (Mise et al., 1996), which was established from a teratocarcinoma by transplantation of an E7.5 mouse embryo into the testis (McBurney and Rogers, 1982). P19 cell line is commonly used to study mechanisms of neurogenesis and myogenesis (Bain et al., 1994; van der Heyden and Defize, 2003), but it possibly have similar characteristics to spermatogenic cells because a factor for germ cell differentiation, *Stra8*, was reported to be induced by retinoic acid (Oulad-Abdelghani et al., 1996). In our assay, some transcription factors that were commonly expressed in the testis and in the two cell lines we used might bind to the flanking sequences to *lncRNA-HSVIII* and enhance *Prss42/Tessp-2* promoter activity.

It is interesting that enhancer activity in the 5.8-kb fragment was divided into two regions: 5' and 3' flanking sequences of *lncRNA-HSVIII* (Fig. 7). This suggests that the upstream and downstream regions of *lncRNA-HSVIII* cooperatively function to enhance *Prss42/Tessp-2* promoter activity, which is reminiscent of super-enhancers (Pott and Lieb, 2014). Super-enhancers were first reported in mouse embryonic stem cells and contained several enhancers, each of which was located within 12.5 kb, to activate genes for cell type specification (Whyte et al., 2013). In a super-enhancer, each enhancer interacts with the target promoter, resulting in the formation of complex chromatin structure. If both 5' and 3' sequences to *lncRNA-HSVIII* enhance *Prss42/Tessp-2* promoter activity in spermatocytes, they may independently interact with the promoter. Alternatively, the 3' sequence to *lncRNA-HSVIII* may mainly function as an enhancer, and the 5' sequence may play an auxiliary role in the *Prss42/Tessp-2* gene regulation. It is unclear whether the flanking sequences to *lncRNA-HSVIII* are parts of a super-enhancer, but we assume that at least the 3' sequence to *lncRNA-HSVIII* is required for activation of the *Prss42/Tessp-2* gene in spermatocytes during germ cell differentiation.

Finally, we discuss the regulatory mechanism of the gene cluster. The gene cluster usually

consists of several paralogues that were generated by duplication of an ancestral gene in the process of evolution. Indeed, the *Prss/Tessp* gene cluster contains three paralogous genes and they were estimated to be generated by gene duplication (Yoneda et al., 2013). As discussed above, our current data demonstrated that the *lncRNA-HSVIII* region interacted with the *Prss42/Tessp-2* promoter but not with promoters of the other cluster genes, which indicates that *Prss/Tessp* cluster genes are controlled by different elements. This is interesting because most gene clusters are controlled together by a single cis-regulatory element such as locus control region (Fraser and Grosveld, 1998; Festenstein and Kioussis, 2000; Sproul et al., 2005; Dean, 2006). Even if cluster genes are expressed at different developmental stages or in different tissues, locus control region regulates the entire cluster (Grosveld et al., 1987; Jones et al., 1995; Su et al., 2000). The regulation of the *Prss/Tessp* gene cluster is in contrast to the mechanism for other gene clusters, because the *Prss42/Tessp-2* gene is possibly regulated by its downstream sequence that possesses enhancer activity, but the sequence does not engage in the regulation of *Prss44/Tessp-4* and *Prss43/Tessp-3* genes. Therefore, our current data also provide a new insight into the regulation of gene clusters.

MATERIALS AND METHODS

Animals

C57BL6/Crj mice (CLEA Japan Inc., Tokyo, Japan) were maintained on 14 hr light/10 hr dark cycles at 25°C, and fed with enough food and water. The experimental procedures used in this study were approved by the Institutional Animal Use and Care Committee at Hokkaido University.

DNase I HS Mapping

Native germ cells were isolated from two adult mouse testes and the purity was checked by the marker gene expression as previously described (Yoneda et al., 2013; Kurihara et al., 2014). The cells

were lysed with 4 ml NP-40 lysis buffer (10 mM Tris-HCl (pH 7.5), 10 mM NaCl, 3 mM MgCl₂, 0.5% NP-40) containing 1×proteinase inhibitor cocktail (Roche Molecular Biochemicals, Mannheim, Germany). Liver nuclei were collected by cutting and homogenizing 0.1 g liver piece in 4 ml NP-40 lysis buffer containing 1×proteinase inhibitor cocktail. The nuclei were collected by centrifugation, washed with 1 ml DNase I digestion buffer (0.1 M NaCl, 50 mM Tris-HCl (pH 7.5), 3 mM MgCl₂, 1 mM CaCl₂, 0.1 mM phenylmethylsulfonyl fluoride), and suspended again in 625 µl DNase I digestion buffer. The suspension was divided into five aliquots, and 125 µl DNase I digestion buffer was added to one aliquot and mixed with 250 µl 2×Stop solution (20 mM Tris-HCl (pH 7.5), 100 mM EDTA, 600 mM NaCl, 1% SDS, 200 µg/ml proteinase K). The remaining four aliquots were mixed with 125 µl DNase I digestion buffer containing 40 U/ml DNase I (Takara, Ohtsu, Japan) and treated for 15, 45, 90, and 180 sec at 37°C. The reaction was stopped by adding 250 µl 2×Stop solution to each sample, and all the five samples were incubated at 55°C for overnight to purify the genome DNA. The aliquot without DNase I digestion was used as a sample at a time point of 0 sec. The purified DNA was measured, and approximately 5-10 µg DNA was digested with restriction enzymes, *Hind*III, *Bam*HI, or *Eco*RI at 37°C for 20 hr and purified by phenol/chloroform isoamylalcohol (CIAA) extraction and ethanol precipitation. These samples were separated by electrophoresis on 0.7% agarose gels and transferred to Hybond-N⁺ membranes (GE Healthcare, Piscataway, USA) for Southern blot hybridization.

Southern Blot Hybridization

A 38-kb region encompassing the *Prss42/Tessp-2* gene was detected as two fragments resulting from *Hind*III and *Bam*HI digestion (Fig. 1A). A 679-bp probe, which could detect both fragments, was prepared by PCR amplification with ExTaq polymerase (Takara) and mouse genome DNA. After the PCR amplification, the products were subcloned into a pBluescript II vector, and their sequences were checked by the DNA sequencing analysis. We selected the clone which contained the completely correct sequence, and by restriction digestion, agarose gel electrophoresis, and DNA purification from

the gel, we obtained the probe. The probe was ^{32}P -labeled and hybridized with the membranes either at 65°C in 0.5 M sodium phosphate (pH 7.2), 0.1 mM EDTA, 5% SDS, 1% bovine serum albumin, and 100 µg/ml herring sperm DNA or at 42°C in 50% formamide, 5×Denhardt's solution, 5×SSPE, 1% SDS, and 100 µg/ml herring sperm DNA. The membranes were washed with 1×SSC/0.1% SDS at 65°C or 50°C, and the signals were detected by autoradiography using Kodak Biomax MR films. For fine mapping of the *Prss42/Tessp-2* promoter region, the genome DNA treated with DNase I was digested with *EcoRI*, and a 711-bp probe for this fragment was obtained as above (Fig. 1A). The primers for PCR reactions to prepare probes are listed in Table 1.

RT-PCR Analysis

Total RNAs were extracted by ISOGEN II (Nippon gene, Tokyo, Japan) according to the manufacturer's instruction. After the treatment with TurboDNase I (Ambion, Austin, USA), RNAs were reverse-transcribed into cDNAs using Superscript III (Invitrogen, Carlsbad, USA) according to the instruction. PCR was performed by using ExTaq polymerase (Takara). Primer sequences are shown in Table 1.

5'RACE and 3'RACE

RACE analyses were performed as previously described (Kurihara et al., 2014; Matsubara et al., 2014). For 5'RACE, reverse transcription was done with RT-1 primer, and the first PCR was performed with GSP1 and Abridged Anchor Primer. The second nested PCR was performed using GSP2 and Abridged Universal Amplification Primer. For 3'RACE, the first and second PCRs were performed using GSP3 and GSP4, respectively, with 3 sites Adaptor Primer. All the products were subcloned into a pBluescript II vector (Stratagene, La Jolla, USA) by the TA-cloning method, and the sequences of at least ten subclones were determined for each experiment. Primer positions are indicated in Fig. 2A and their sequences are shown in Table 1.

Preparation of Germ, Sertoli, and Sertoli/Leydig Cell Fractions

The germ cell fraction was prepared as above. The Sertoli cell fraction was obtained from 11-day-old testes by primary culture of Sertoli cells as previously described (Yoneda and Kimura, 2013). The Sertoli/Leydig cell fraction was obtained from 6-month-old testes as follows. The testes were decapsulated and treated with 0.1% collagenase at 32°C. The floating cells were collected and applied to discontinuous Percoll gradient (20%, 37%, and 53%). After centrifugation, the cells between 37% and 53% were washed and used as the Sertoli/Leydig cell fraction.

Preparation of Subcellular Fractions

Testicular germ cells were lysed in NP-40 lysis buffer on ice for 10 min, and the lysate was centrifuged at 1500 rpm for 5 min at 4°C. The supernatant was used as the cytoplasmic fraction, and the precipitates were washed with the same buffer 2-3 times. The resulting pellet was used as the nuclear fraction.

In situ Hybridization

For in situ hybridization analysis, adult mouse testes were fixed with 4% paraformaldehyde in phosphate buffered saline (PBS) for 3 hr at 4°C. The tissues were washed three times with PBS and dissected into two pieces with a razor blade under a dissecting microscope. In situ hybridization with the TSA Plus system (PerkinElmer) was performed according to the procedure reported previously (Kotani et al., 2013). Briefly, samples were dehydrated, embedded in paraffin, and cut into 7- μ m-thick sections. The sense and antisense RNA probes for *lncRNA-HSVIII* were synthesized with digoxigenin (DIG) RNA labeling kit (Roche Molecular Biochemicals). This time, we used a full-length sequence of *lncRNA-HSVIII* (2665 nucleotides) for labeling. After hybridization and washing, the sections were incubated with anti-DIG-horseradish peroxidase antibody (Roche Molecular Biochemicals) (1:500 dilution) for 30 min. The reaction with tyramide-Cy3 was performed according to the manufacturer's instructions. After the incubation with 10 μ g/ml Hoechst 33258 for 10 min, the samples were observed

under an LSM5LIVE confocal microscope (Carl Zeiss).

Fractionation of Germ Cells into Different Meiotic Stages

Testicular germ cells were fractionated into different meiotic stages by a cell sorter as previously described (Yoneda et al., 2013).

3C Assay

3C assay was performed according to previously published methods with modifications (Hagège et al., 2007; Ho et al., 2008). Native testicular germ cells were obtained as above, and hepatic cells were collected by homogenization of a 0.1 g liver piece in Opti-MEM (Invitrogen). The cells were crosslinked by 1% formaldehyde in Opti-MEM for 10 min, and the crosslink reaction was stopped by adding glycine solution at a final concentration of 0.125 M and incubating the sample for 5 min. After being washed twice with ice-cold PBS, the cells were suspended in 1 ml ice-cold PBS containing 1×proteinase inhibitor cocktail (Roche Molecular Biochemicals) and centrifuged at 700×g at 4°C for 5 min. By suspending the cells in Cold Lysis buffer (10 mM Tris-HCl (pH 7.5), 10 mM NaCl, 5 mM MgCl₂, 1×proteinase inhibitor, 0.2% NP-40) and incubating on ice for 10 min, the crosslinked nuclei were centrifuged at 420×g at 4°C for 5 min. After being washed with ice-cold PBS, the nuclei were suspended in the mixture of 1.2×H buffer (Takara) and 0.1% SDS and incubated at 37°C for 1 hr while shaking at 200 rpm. Then, Triton-X100 was added to the samples at a final concentration of 2% to neutralize SDS, and the mixture was incubated at 37°C for 1 hr while shaking at 200 rpm. 2000 units of *Pst*I (Takara, high concentration) were added to the nuclei and were incubated at 37°C for overnight while shaking at 200 rpm. At this point, the concentration of H buffer became 1×. After the restriction digestion, SDS was added at a final concentration of 1.67% to the reaction, and the sample was incubated at 65°C for 30 min. Then, the sample was split into two portions (one for ligation and the other for negative control), and each of them was mixed with 1×Takara ligation buffer (66 mM Tris-HCl (pH 7.5), 6.6 mM MgCl₂, 10mM DTT, 0.1 mM ATP) to dilute it to approximately 10 times

and with Triton-X100 at a final concentration of 1% to neutralize SDS. After incubation at 37°C for 30 min while shaking at 120 rpm, 1500 units of T4 DNA Ligase (Takara) was added to one portion, and the samples were incubated at 16°C for 4 hr while shaking at 60 rpm, followed by incubation at room temperature for 1 hr. After the ligation, proteinase K was added at a final concentration of 20 µg/ml and the samples were incubated at 65°C for overnight to reverse-crosslink the chromatin and to digest proteins. The samples were purified by phenol/CIAA extraction and ethanol precipitation, and finally dissolved in TE.

As a positive control, 10 µg of BAC DNA encompassing the *Prss/Tessp* gene cluster (B6Ng01-306015, RIKEN Bioresource Center, Tsukuba, Japan) were digested with 25 units of *PstI* at 37°C for 2 hr. The digested DNA was purified by phenol/CIAA extraction and ethanol precipitation, and ligated with 50 units of T4 DNA Ligase in 1×Takara ligation buffer at 16°C for 4 hr. The ligated DNA was purified by phenol/CIAA extraction and ethanol precipitation, and dissolved in TE.

3C PCR primers were designed around *PstI* restriction sites at or close to HSI, HSIV, *Prss42/Tessp-2* promoter, *Prss44/Tessp-4* promoter, 3' end of *Prss44/Tessp-4*, an intergenic region between *Prss44/Tessp-4* and *Prss43/Tessp-3*, and *Prss43/Tessp-3* promoter in an antisense orientation (Fig. 4A). The anchor primer was designed at 3' of the *lncRNA-HSVIII* sequence in a sense orientation. Quantitative PCR was conducted with KOD SYBR qPCR Mix (Toyobo, Tokyo, Japan) under the condition of 40 cycles of 98°C for 10 sec, 60°C for 10 sec, and 68°C for 1 min. The data was first normalized to those with the BAC clone to equalize the relative PCR efficiency, and interaction frequencies were further normalized to that at the *Erc3* gene locus, which was expected to show similar interaction frequency irrespective of cell- and tissue-types (Palstra et al., 2003). All the primers used for 3C assay are listed in Table 1.

Plasmid Constructs

The *Prss42/Tessp-2* promoter sequence was amplified by PCR with mouse genome DNA using KOD polymerase (Toyobo) and a primer pair listed in Table 1. The 1636-bp product was blunted and

phosphorylated, and inserted into a pGL-3 Basic vector (Promega Corporation, Madison, USA) at the blunted *HindIII* site. We used the plasmid clone which contained no mutation in the promoter after checking the sequence. The 5.8-kb fragment encompassing the *lncRNA-HSVIII* sequence was obtained by digestion of a mouse BAC clone, B6Ng01-306015 (RIKEN Bioresource Center), with *EcoRI*, and subcloned into a pBluescript II vector (Stratagene). The fragment was further cut out from the vector with *EcoRI*, blunted and phosphorylated, and inserted into the pGL-3 Basic vector containing the *Prss42/Tessp-2* promoter at the blunted *BamHI* site. A 6.7-kb λ *HindIII* fragment was obtained from a λ *HindIII* marker and inserted into the same vector at the blunted *BamHI* site after blunted and phosphorylated.

To obtain the full-length sequence of *lncRNA-HSVIII*, we first amplified 2562-bp 5'-half and 259-bp 3'-half of this lncRNA, separately, by RT-PCR using primer pairs shown in Table 1. The two products were separately subcloned into a pBluescript II KS(+) vector at the *EcoRV* site by the TA-cloning method, and their sequences were confirmed by DNA sequencing. Then, we digested both plasmids with *BglII* and *SalI*, and inserted a 109-bp 3'-half into the plasmid containing a 2556-bp 5'-half. After digestion of the plasmid which contained the full-length of *lncRNA-HSVIII* with *BamHI* and *SalI*, we ligated the *lncRNA-HSVIII* fragment into *BamHI/SalI* site of the pGL-3 Basic vector containing the *Prss42/Tessp-2* promoter. Alternatively, the digested *lncRNA-HSVIII* fragment was blunted and phosphorylated, and inserted into the *SmaI* site of the construct.

To obtain upstream and downstream sequences of *lncRNA-HSVIII*, we digested the pBluescript vector containing the 5.8-kb fragment with *SmaI/HincII* and *SacI/EcoRV*, respectively. The fragments were blunted and phosphorylated, and inserted into the blunted *BamHI* site of the pGL-3 Basic vector containing the *Prss42/Tessp-2* promoter.

Cell Culture, Transfection, and Reporter Gene Assay

Hepa1-6 cells were cultured as previously described (Matsubara et al., 2010). P19TG1 cells were cultured with Eagle's minimum essential medium containing fetal bovine serum (10%) and

L-glutamine (2 mM) in the 37°C incubator supplied with 5% CO₂.

Because molecular weights were greatly different between constructs, we used the same molar amount of DNA in each assay. For reporter assay, Hepa1-6 cells were cultured in 24-well dishes and transfected with constructs by using the GeneJuice reagent (Novagen, Madison, USA) according to the instruction. P19TG1 cells were cultured in 35-mm dishes and transfected by using the FuGENE-HD reagent (Promega Corporation). The day before transfection, 0.5×10^5 P19TG1 cells were seeded on a 35-mm dish. On the day of transfection, the cell confluency was about 50-80%, and we formed complexes of various constructs with FuGENE-HD transfection reagent and added them to cells, according to manufacturer's instructions. The cells were collected 48 hours after transfection, and luciferase activity was measured by using Dual-Luciferase Reporter Assay System (Promega Corporation).

The construct we prepared as above contained the *Firefly* luciferase gene, and in each experiment, we co-transfected it with a pRL-CMV vector (Promega Corporation) in which the *Renilla* luciferase gene was driven by the CMV promoter. All the constructs were transfected as circular plasmids. We normalized *Firefly* luciferase activity to *Renilla* luciferase activity for adjusting transfection efficiency. The activity was further normalized to that of the cells transfected with a pGL3-Basic vector, and relative activity was calculated as the value from a pGL3-Basic vector was set to 1.0.

Statistical Analysis

Results were expressed as the average \pm standard deviation (SD) of at least three independent experiments. Student's *t*-test and Dunnett's test were performed using Microsoft Excel statistical analysis functions (Microsoft Corporation, Redmond, USA). Differences were considered statistically significant at $P < 0.05$.

ACKNOWLEDGEMENTS

We thank Dr. Masatoshi Matsunami for helping us to analyze transcriptomic data.

REFERENCES

- Alabert C, Groth A. 2012. Chromatin replication and epigenome maintenance. *Nat Rev Mol Cell Biol* **13**:153–67.
- Arvey A, Agius P, Noble WS, Leslie C. 2012. Sequence and chromatin determinants of cell-type-specific transcription factor binding. *Genome Res* **22**:1723–34.
- Atianand MK, Fitzgerald KA. 2014. Long non-coding RNAs and control of gene expression in the immune system. *Trends Mol Med* **20**:623–31.
- Bain G, Ray WJ, Yao M, Gottlieb DI. 1994. From embryonal carcinoma cells to neurons: the P19 pathway. *Bioessays* **16**:343–8.
- Bao J, Wu J, Schuster AS, Hennig GW, Yan W. 2013. Expression Profiling Reveals Developmentally Regulated lncRNA Repertoire in the Mouse Male Germline. *Biol Reprod* **89**:107.
- Bartkuhn M, Renkawitz R. 2008. Long range chromatin interactions involved in gene regulation. *Biochim Biophys Acta* **1783**:2161–6.
- Chen L-L, Carmichael GG. 2010. Decoding the function of nuclear long non-coding RNAs. *Curr Opin Cell Biol* **22**:357–64.
- Cockerill PN. 2011. Structure and function of active chromatin and DNase I hypersensitive sites. *FEBS J* **278**:2182–210.
- Darlington GJ. 1987. Liver cell lines. *Methods Enzymol* **151**:19–38.
- Darlington GJ, Bernhard HP, Miller RA, Ruddle FH. 1980. Expression of liver phenotypes in cultured mouse hepatoma cells. *J Natl Cancer Inst* **64**:809–19.
- Dean A. 2006. On a chromosome far, far away: LCRs and gene expression. *Trends Genet* **22**:38–45.
- DeJong J. 2006. Basic mechanisms for the control of germ cell gene expression. *Gene* **366**:39–50.
- Dekker J, Rippe K, Dekker M, Kleckner N. 2002. Capturing chromosome conformation. *Science* **295**:1306–11.
- Festenstein R, Kioussis D. 2000. Locus control regions and epigenetic chromatin modifiers. *Curr Opin*

- Genet Dev* **10**:199–203.
- Fraser P, Grosveld F. 1998. Locus control regions, chromatin activation and transcription. *Curr Opin Cell Biol* **10**:361–5.
- Ghirlando R, Giles K, Gowher H, Xiao T, Xu Z, Yao H, Felsenfeld G. 2012. Chromatin domains, insulators, and the regulation of gene expression. *Biochim Biophys Acta* **1819**:644–51.
- Goldberg E, Eddy EM, Duan C, Odet F. 2010. LDHC: the ultimate testis-specific gene. *J Androl* **31**:86–94.
- Goodrich JA, Tjian R. 2010. Unexpected roles for core promoter recognition factors in cell-type-specific transcription and gene regulation. *Nat Rev Genet* **11**:549–58.
- Grimes SR. 2004. Testis-specific transcriptional control. *Gene* **343**:11–22.
- Grosveld F, van Assendelft GB, Greaves DR, Kollias G. 1987. Position-independent, high-level expression of the human β -globin gene in transgenic mice. *Cell* **51**:975–985.
- Hagège H, Klous P, Braem C, Splinter E, Dekker J, Cathala G, de Laat W, Forné T. 2007. Quantitative analysis of chromosome conformation capture assays (3C-qPCR). *Nat Protoc* **2**:1722–33.
- Han S, Xie W, Kim SH, Yue L, DeJong J. 2004. A short core promoter drives expression of the ALF transcription factor in reproductive tissues of male and female mice. *Biol Reprod* **71**:933–41.
- Ho Y, Tadevosyan A, Liebhaber SA, Cooke NE. 2008. The juxtaposition of a promoter with a locus control region transcriptional domain activates gene expression. *EMBO Rep* **9**:891–8.
- Hofmann MC, Hess RA, Goldberg E, Millán JL. 1994. Immortalized germ cells undergo meiosis in vitro. *Proc Natl Acad Sci U S A* **91**:5533–7.
- Iwafuchi-Doi M, Zaret KS. 2014. Pioneer transcription factors in cell reprogramming. *Genes Dev* **28**:2679–2692.
- Jenuwein T, Allis CD. 2001. Translating the histone code. *Science* **293**:1074–80.
- Johnston DS, Wright WW, Dicandoloro P, Wilson E, Kopf GS, Jelinsky SA. 2008. Stage-specific gene expression is a fundamental characteristic of rat spermatogenic cells and Sertoli cells. *Proc Natl Acad Sci U S A* **105**:8315–20.
- Jones BK, Monks BR, Liebhaber SA, Cooke NE. 1995. The human growth hormone gene is regulated by a multicomponent locus control region. *Mol Cell Biol* **15**:7010–21.
- Kehoe SM, Oka M, Hankowski KE, Reichert N, Garcia S, McCarrey JR, Gaubatz S, Terada N. 2008. A conserved E2F6-binding element in murine meiosis-specific gene promoters. *Biol Reprod* **79**:921–30.

- Kotani T, Yasuda K, Ota R, Yamashita M. 2013. Cyclin B1 mRNA translation is temporally controlled through formation and disassembly of RNA granules. *J Cell Biol* **202**:1041–55.
- Kramer J, McCarrey J, Djakiew D, Krawetz S. 1998. Differentiation: the selective potentiation of chromatin domains. *Development* **125**:4749–4755.
- Kumari M, Stroud JC, Anji A, McCarrey JR. 1996. Differential appearance of DNase I-hypersensitive sites correlates with differential transcription of P_{gk} genes during spermatogenesis in the mouse. *J Biol Chem* **271**:14390–7.
- Kurihara M, Shiraishi A, Satake H, Kimura AP. 2014. A conserved noncoding sequence can function as a spermatocyte-specific enhancer and a bidirectional promoter for a ubiquitously expressed gene and a testis-specific long noncoding RNA. *J Mol Biol* **426**:3069–93.
- Lai F, Orom UA, Cesaroni M, Beringer M, Taatjes DJ, Blobel GA, Shiekhattar R. 2013. Activating RNAs associate with Mediator to enhance chromatin architecture and transcription. *Nature* **494**:497–501.
- Langford KG, Zhou Y, Russell LD, Wilcox JN, Bernstein KE. 1993. Regulated expression of testis angiotensin-converting enzyme during spermatogenesis in mice. *Biol Reprod* **48**:1210–8.
- Lele KM, Wolgemuth DJ. 2004. Distinct regions of the mouse cyclin A1 gene, *Ccna1*, confer male germ-cell specific expression and enhancer function. *Biol Reprod* **71**:1340–7.
- Li S, Zhou W, Doglio L, Goldberg E. 1998. Transgenic mice demonstrate a testis-specific promoter for lactate dehydrogenase, LDHC. *J Biol Chem* **273**:31191–4.
- Li W, Notani D, Ma Q, Tanasa B, Nunez E, Chen AY, Merkurjev D, Zhang J, Ohgi K, Song X, Oh S, Kim H-S, Glass CK, Rosenfeld MG. 2013. Functional roles of enhancer RNAs for oestrogen-dependent transcriptional activation. *Nature* **498**:516–20.
- Liang M, Li W, Tian H, Hu T, Wang L, Lin Y, Li Y, Huang H, Sun F. 2014. Sequential expression of long noncoding RNA as mRNA gene expression in specific stages of mouse spermatogenesis. *Sci Rep* **4**:5966.
- Martins RP, Krawetz SA. 2007. Decondensing the protamine domain for transcription. *Proc Natl Acad Sci U S A* **104**:8340–5.
- Matsubara S, Kurihara M, Kimura AP. 2014. A long non-coding RNA transcribed from conserved non-coding sequences contributes to the mouse prolyl oligopeptidase gene activation. *J Biochem* **155**:243–56.
- Matsubara S, Takahashi T, Kimura AP. 2010. Epigenetic patterns at the mouse prolyl oligopeptidase gene locus suggest the CpG island in the gene body to be a novel regulator for gene expression. *Gene* **465**:17–29.

- McBurney MW, Rogers BJ. 1982. Isolation of male embryonal carcinoma cells and their chromosome replication patterns. *Dev Biol* **89**:503–8.
- Mercer TR, Edwards SL, Clark MB, Neph SJ, Wang H, Stergachis AB, John S, Sandstrom R, Li G, Sandhu KS, Ruan Y, Nielsen LK, Mattick JS, Stamatoyannopoulos JA. 2013. DNase I-hypersensitive exons colocalize with promoters and distal regulatory elements. *Nat Genet* **45**:852–9.
- Mise N, Sado T, Tada M, Takada S, Takagi N. 1996. Activation of the inactive X chromosome induced by cell fusion between a murine EC and female somatic cell accompanies reproducible changes in the methylation pattern of the Xist gene. *Exp Cell Res* **223**:193–202.
- Morales CR, Kwon YK, Hecht NB. 1991. Cytoplasmic localization during storage and translation of the mRNAs of transition protein 1 and protamine 1, two translationally regulated transcripts of the mammalian testis. *J Cell Sci* **100** (Pt 1):119–31.
- Natarajan A, Yardimci GG, Sheffield NC, Crawford GE, Ohler U. 2012. Predicting cell-type-specific gene expression from regions of open chromatin. *Genome Res* **22**:1711–22.
- Necsulea A, Soumillon M, Warnefors M, Liechti A, Daish T, Zeller U, Baker JC, Grützner F, Kaessmann H. 2014. The evolution of lncRNA repertoires and expression patterns in tetrapods. *Nature* **505**:635–40.
- Ou C-M, Lin S-R, Lin H-J, Luo C-W, Chen Y-H. 2010. Exclusive expression of a membrane-bound Spink3-interacting serine protease-like protein TESPL in mouse testis. *J Cell Biochem* **110**:620–9.
- Oulad-Abdelghani M, Bouillet P, Décimo D, Gansmuller A, Heyberger S, Dollé P, Bronner S, Lutz Y, Chambon P. 1996. Characterization of a premeiotic germ cell-specific cytoplasmic protein encoded by Stra8, a novel retinoic acid-responsive gene. *J Cell Biol* **135**:469–77.
- Palstra R-J, Tolhuis B, Splinter E, Nijmeijer R, Grosveld F, de Laat W. 2003. The beta-globin nuclear compartment in development and erythroid differentiation. *Nat Genet* **35**:190–4.
- Peschon JJ, Behringer RR, Brinster RL, Palmiter RD. 1987. Spermatid-specific expression of protamine 1 in transgenic mice. *Proc Natl Acad Sci U S A* **84**:5316–9.
- Peschon JJ, Behringer RR, Palmiter RD, Brinster RL. 1989. Expression of mouse protamine 1 genes in transgenic mice. *Ann N Y Acad Sci* **564**:186–97.
- Ponting CP, Oliver PL, Reik W. 2009. Evolution and functions of long noncoding RNAs. *Cell* **136**:629–41.
- Pott S, Lieb JD. 2014. What are super-enhancers? *Nat Genet* **47**:8–12.
- Reddi PP, Flickinger CJ, Herr JC. 1999. Round spermatid-specific transcription of the mouse SP-10

- gene is mediated by a 294-base pair proximal promoter. *Biol Reprod* **61**:1256–66.
- Reddi PP, Urekar CJ, Abhyankar MM, Ranpura SA. 2007. Role of an insulator in testis-specific gene transcription. *Ann N Y Acad Sci* **1120**:95–103.
- Rinn JL, Chang HY. 2012. Genome regulation by long noncoding RNAs. *Annu Rev Biochem* **81**:145–66.
- Robinson MO, McCarrey JR, Simon MI. 1989. Transcriptional regulatory regions of testis-specific PGK2 defined in transgenic mice. *Proc Natl Acad Sci U S A* **86**:8437–41.
- Sanyal A, Lajoie BR, Jain G, Dekker J. 2012. The long-range interaction landscape of gene promoters. *Nature* **489**:109–13.
- Schäfer M, Nayernia K, Engel W, Schäfer U. 1995. Translational control in spermatogenesis. *Dev Biol* **172**:344–52.
- Shima JE, McLean DJ, McCarrey JR, Griswold MD. 2004. The murine testicular transcriptome: characterizing gene expression in the testis during the progression of spermatogenesis. *Biol Reprod* **71**:319–30.
- Simpson AJG, Caballero OL, Jungbluth A, Chen Y-T, Old LJ. 2005. Cancer/testis antigens, gametogenesis and cancer. *Nat Rev Cancer* **5**:615–25.
- Sipos L, Gyurkovics H. 2005. Long-distance interactions between enhancers and promoters. *FEBS J* **272**:3253–9.
- Sproul D, Gilbert N, Bickmore WA. 2005. The role of chromatin structure in regulating the expression of clustered genes. *Nat Rev Genet* **6**:775–81.
- Su Y, Liebhaber SA, Cooke NE. 2000. The human growth hormone gene cluster locus control region supports position-independent pituitary- and placenta-specific expression in the transgenic mouse. *J Biol Chem* **275**:7902–9.
- Sun J, Lin Y, Wu J. 2013. Long non-coding RNA expression profiling of mouse testis during postnatal development. *PLoS One* **8**:e75750.
- Todeschini A-L, Georges A, Veitia RA. 2014. Transcription factors: specific DNA binding and specific gene regulation. *Trends Genet* **30**:211–9.
- Tolhuis B, Palstra RJ, Splinter E, Grosveld F, de Laat W. 2002. Looping and interaction between hypersensitive sites in the active beta-globin locus. *Mol Cell* **10**:1453–65.
- Umlauf D, Fraser P, Nagano T. 2008. The role of long non-coding RNAs in chromatin structure and gene regulation: variations on a theme. *Biol Chem* **389**:323–31.
- van der Heyden MAG, Defize LHK. 2003. Twenty one years of P19 cells: what an embryonal carcinoma cell line taught us about cardiomyocyte differentiation. *Cardiovasc Res* **58**:292–302.

- Wang KC, Chang HY. 2011. Molecular mechanisms of long noncoding RNAs. *Mol Cell* **43**:904–14.
- Wang PJ, Page DC, McCarrey JR. 2005. Differential expression of sex-linked and autosomal germ-cell-specific genes during spermatogenesis in the mouse. *Hum Mol Genet* **14**:2911–8.
- Whyte WA, Orlando DA, Hnisz D, Abraham BJ, Lin CY, Kagey MH, Rahl PB, Lee TI, Young RA. 2013. Master transcription factors and mediator establish super-enhancers at key cell identity genes. *Cell* **153**:307–19.
- Wilusz JE, Sunwoo H, Spector DL. 2009. Long noncoding RNAs: functional surprises from the RNA world. *Genes Dev* **23**:1494–504.
- Wu X, Brewer G. 2012. The regulation of mRNA stability in mammalian cells: 2.0. *Gene* **500**:10–21.
- Xiang J-F, Yin Q-F, Chen T, Zhang Y, Zhang X-O, Wu Z, Zhang S, Wang H-B, Ge J, Lu X, Yang L, Chen L-L. 2014. Human colorectal cancer-specific CCAT1-L lncRNA regulates long-range chromatin interactions at the MYC locus. *Cell Res* **24**:513–31.
- Yan W, Si Y, Slaymaker S, Li J, Zheng H, Young DL, Aslanian A, Saunders L, Verdin E, Charo IF. 2010. Zmynd15 encodes a histone deacetylase-dependent transcriptional repressor essential for spermiogenesis and male fertility. *J Biol Chem* **285**:31418–26.
- Yoneda R, Kimura AP. 2013. A testis-specific serine protease, Prss41/Tessp-1, is necessary for the progression of meiosis during murine in vitro spermatogenesis. *Biochem Biophys Res Commun* **441**:120–5.
- Yoneda R, Takahashi T, Matsui H, Takano N, Hasebe Y, Ogiwara K, Kimura AP. 2013. Three testis-specific paralogous serine proteases play different roles in murine spermatogenesis and are involved in germ cell survival during meiosis. *Biol Reprod* **88**:118.
- Zambrowicz BP, Harendza CJ, Zimmermann JW, Brinster RL, Palmiter RD. 1993. Analysis of the mouse protamine 1 promoter in transgenic mice. *Proc Natl Acad Sci U S A* **90**:5071–5.
- Zaratiegui M, Irvine D V, Martienssen RA. 2007. Noncoding RNAs and gene silencing. *Cell* **128**:763–76.

FIGURE LEGENDS

Figure 1. DNase I HS mapping at the mouse *Prss/Tessp* locus. **A:** Schematic drawing of the *Prss/Tessp* gene cluster showing the position of identified DNase I HSs in germ cells and liver cells by

vertical arrows. A 63-kb region corresponding to 110775-110838 kb of the mouse chromosome 9 is drawn. The width of the arrow reflects the signal intensity of each DNase I HS. Three cluster genes are depicted with white boxes and bent arrows indicate the transcriptional direction. An about 38-kb sequence encompassing the *Prss42/Tessp-2* gene was searched as three restriction fragments digested with *Bam*HI, *Hind*III, or *Eco*RI. Restriction sites and fragment sizes are shown below the gene structure. **B:** Southern blot analysis detecting DNase I HSs on the *Hind*III fragment. Nuclei from native testicular germ cells and liver cells were treated with DNase I for 0, 15, 45, 90, or 180 sec, and genome DNAs were purified. After digestion with *Hind*III, DNAs were transferred to a nylon membrane and hybridized with a radio-labeled probe (a grey box). The membrane was washed, and signals were detected by autoradiography. The *Prss42/Tessp-2* gene and its upstream region are drawn at the top with the *Hind*III fragment and the fragments detected as a result of DNase I treatment. Sizes of DNase I-digested fragments are shown, and positions of DNase I HSs are indicated with their numbers by vertical arrows. Below the structure, the image of the Southern blot analysis are presented, and the bands corresponding to DNase I HSs are indicated by horizontal arrows. Molecular size markers are shown at right. **C:** Southern blot analysis detecting DNase I HSs on the *Bam*HI fragment. DNase I treatment and Southern blot analysis were performed as in **B**, and the structure of the *Prss42/Tessp-2* and *Prss44/Tessp-4* locus and the Southern blot image are indicated as in **B**. An arrowhead shows the signal which was not detected by *Eco*RI digestion in liver cells. **D:** Fine mapping of the *Prss42/Tessp-2* promoter region. DNase I treatment of nuclei, restriction digestion with *Eco*RI, and Southern blot were performed as in **B**. A promoter region and the first four exons of the *Prss42/Tessp-2* gene are drawn at the top. Positions of DNase I HSs are indicated by vertical arrows, and exons are depicted with white boxes connected by bent lines. Below the gene structure, an *Eco*RI fragment is shown with the fragments detected after DNase I treatment, and the probe for Southern blot is indicated by a grey box. The Southern blot image is presented as in **B**.

Figure 2. Characterization and expression of *lncRNA-HSVIII*. **A:** Schematic drawing of the

Prss42/Tessp-2 gene and *lncRNA-HSVIII*. Exons of the *Prss42/Tessp-2* gene are depicted with black and white boxes. A black box represent a coding region and a white box represents an untranslated region. *lncRNA-HSVIII* contains no intron. Bent arrows indicate the transcriptional direction of the *Prss42/Tessp-2* gene and *lncRNA-HSVIII*. A vertical arrow shows the position of DNase I HSVIII.

Below the structure, primer positions used in 5'RACE and 3' RACE are indicated by short horizontal arrows. **B:** Tissue specificity of *lncRNA-HSVIII* was examined by RT-PCR. Total RNAs were isolated from eight mouse tissues as indicated, and reverse transcription was performed using the oligo(dT) primer with (RT+) or without reverse transcriptase (RT-). The cycle number of each PCR reaction is indicated in the parenthesis at right. The *Gapdh* gene was examined as an internal control.

lncRNA-HSVIII was specifically expressed in the testis. **C:** Localization of *lncRNA-HSVIII* in the mouse testis was examined by RT-PCR using cDNAs obtained from fractionated native testicular cells. Germ cell fraction and Sertoli/Leydig cell fraction were isolated from adult mouse testes, while Sertoli cells were collected by primary culture of the cells from immature testes. The expression of marker genes was investigated by quantitative RT-PCR and the results are presented in Figure S2. RT-PCR was performed as in **B**, and the cycle number of each PCR is indicated in the parenthesis at right.

lncRNA-HSVIII was mainly expressed in germ cells and at a lower level in Leydig cells. **D:** Subcellular localization of *lncRNA-HSVIII*. Native testicular germ cells were fractionated into the nucleus and cytoplasm, and RT-PCR was performed as in **B**. Two sets of primers were used to check the quality of the two fractions. *Gapdh* (in5-ex6) was amplified to detect immature mRNA in the nucleus, and *Gapdh* (ex5-ex6) was for mature mRNA in the cytoplasm. These two sets of PCR indicate that our subcellular fractionation was successful. The *lncRNA-HSVIII* signal was detected in both fractions, but the nuclear signal was stronger.

Figure 3. Localization of *lncRNA-HSVIII* in the mouse testis. In situ hybridization analysis of *lncRNA-HSVIII* in the adult mouse testis was performed with the TSA system. The testis was fixed with paraformaldehyde, embedded in paraffin, and cut into 7- μ m sections. The sections were

hybridized with DIG-labelled sense or antisense probe for *lncRNA-HSVIII* and subsequently incubated with anti-DIG-HRP antibody. The positive signals were detected as red dots by the reaction with tyramide-Cy3, and nuclei were stained with Hoechst33258 (blue). **A:** A picture of the testis section hybridized with the antisense probe of *lncRNA-HSVIII*. Positive signals (red dots) were observed in all seminiferous tubules and in interstitial Leydig cells. **B:** A picture of the testis section hybridized with the sense probe of *lncRNA-HSVIII*. Few red dots may be seen. **C:** An enlarged picture of Leydig cells on the section hybridized with the antisense probe. Positive red signals were present in both nuclei and cytosols of Leydig cells (red dots pointed by arrows). **D-F:** Enlarged pictures of seminiferous tubules at different stages. Stages are indicated in the pictures. Positive red signals were observed in nuclei of most pachytene spermatocytes and in cytosols of spermatids and some pachytene cells. The cytosolic signals in pachytene spermatocytes are indicated by arrowheads in **F**. All scale bars represent 50 μm .

Figure 4. Spermatocyte-specific interaction of the chromatin at *lncRNA-HSVIII* with the *Prss42/Tessp-2* promoter. **A:** Schematic drawing of primer positions and restriction sites for 3C analysis. The *Prss/Tessp* cluster was depicted with eight DNase I HSs and *lncRNA-HSVIII* at the top. Bent arrows indicate the transcriptional direction and vertical arrows represent DNase I HSs. Below the structure, positions of *PstI* restriction sites are indicated by vertical lines. Between the lines, primer positions are shown by horizontal arrows. An anchor primer is drawn by a black arrow, and the others by grey arrows. Distance from the restriction site close to the anchor primer is indicated at the bottom. **B:** Physical interaction was investigated by 3C analysis in testicular germ cells and liver cells. The cells were crosslinked with formaldehyde, and the nuclei were isolated and digested with *PstI* restriction enzyme. After dilution of the sample, the chromatin was ligated, and genome DNA was purified. Quantitative PCR was performed using the anchor primer at a 3' region of *lncRNA-HSVIII* with another primer at HSI, HSIV, *Prss/Tessp* promoters, and some other regions as indicated in **A**. *PstI* digestion and ligation was also performed with a BAC clone encompassing the *Prss/Tessp* cluster, and the data obtained from germ and hepatic cells were normalized to those from the BAC clone. To

compare the interaction frequency from different tissues, the data were further normalized to those at the *Erc3* locus which was set to 1.0. The black bar represents the position of the anchor primer. The *lncRNA-HSVIII* region interacted with HSIV and the *Prss42/Tessp-2* promoter only in germ cells. The data are presented as mean \pm SD from three independent experiments. * $P < 0.05$ and ** $P < 0.01$ relative to the interaction frequency in liver cells. $P = 0.0475$ at HSVI and 0.0056 at the *Prss42/Tessp-2* promoter. **C:** 3C analysis was conducted with sorted testicular germ cells. Testicular germ cells were fractionated into spermatogonia, primary spermatocytes, secondary spermatocytes, and spermatids/spermatozoa by a cell sorter. 2×10^5 cells were collected for each fraction. 3C assay was conducted and the results are shown as in **B**. * $P < 0.05$, ** $P < 0.01$, and *** $P < 0.001$ relative to the interaction frequency in spermatogonia. $P = 0.00086$ at HSVI in primary spermatocytes, 0.013 at HSVI in secondary spermatocytes, 0.0052 at the *Prss42/Tessp-2* promoter in primary spermatocytes, and 0.041 at the *Prss42/Tessp-2* promoter in secondary spermatocytes.

Figure 5. Enhancer activity of the 5.8-kb sequence encompassing *lncRNA-HSVIII*. **A:** Schematic drawing of the *Prss42/Tessp-2* gene and *lncRNA-HSVIII*. The *Prss42/Tessp-2* locus is drawn as in Fig. 2A. The position of DNase I HSVIII is shown by a vertical arrow. A 5.8-kb *EcoRI* fragment encompassing *lncRNA-HSVIII* is indicated below the gene structure. *HincII* and *SacI* were used to obtain 5' and 3' flanking sequences to *lncRNA-HSVIII*, respectively, and their sizes are shown. **B and C:** Luciferase assay was conducted with constructs indicated at the left side of the graph. The indicated constructs were prepared and transfected into embryonal carcinoma, P19TG1 cells (**B**) or hepatic tumor, Hepa1-6 cells (**C**), and luciferase activity was measured 48 hr after transfection. The value from the construct without any promoter was set to 1.0 in each experiment. The 5.8-kb sequence significantly increased *Prss42/Tessp-2* promoter activity in both cells. The data are presented as mean \pm SD from at least three independent experiments. * $P < 0.05$ relative to the construct without the 5.8-kb sequence and to the construct with a 6.7-kb λ DNA.

Figure 6. No induction of *lncRNA-HSVIII* transcription by the reporter construct. The expression of *lncRNA-HSVIII* was measured by quantitative RT-PCR with cDNAs obtained from P19TG1 cells that were transfected with the indicated constructs. The transfection of the construct with the 5.8-kb fragment did not result in the increase of the *lncRNA-HSVIII* level.

Figure 7. Enhancer activity of upstream and downstream sequences of *lncRNA-HSVIII*. **A:** Enhancer activity of the *lncRNA-HSVIII* sequence was assessed by reporter gene assay. Constructs indicated at the left side of the graph were transfected into P19TG1 cells (top) or Hepa1-6 cells (bottom), and luciferase activity was measured 48 hr after transfection. Relative activity was calculated and presented as in Fig. 5. The *lncRNA-HSVIII* sequence did not possess enhancer activity in either cells. The data are presented as mean \pm SD from at least three independent experiments. **B:** Enhancer activity of the upstream and downstream sequence of *lncRNA-HSVIII* was evaluated. A 2.3-kb upstream and a 1.5-kb downstream sequence of *lncRNA-HSVIII* was obtained by *HincII* and *SacI* restriction digestion of the 5.8-kb fragment, respectively, as indicated in Fig. 5A. All the constructs were separately transfected into P19TG1 cells and Hepa1-6 cells, and luciferase activity was measured and presented as in Fig. 5. Both upstream and downstream sequences significantly increased *Prss42/Tessp-2* promoter activity in both cells. The data are presented as mean \pm SD from at least three independent experiments. * $P < 0.05$ relative to the construct without the 5.8-kb sequence.

TABLE 1. Primers Used in This Study

Designation	Forward	Reverse
DNase I hypersensitive site mapping		
Probe for <i>Bam</i> HI and <i>Hind</i> III fragments	5'-GGC AAT CTC TGA TCT TAC CC-3'	5'-ACA GCA AGG AAC TCC TGA CA-3'
Probe for <i>Eco</i> RI fragment	5'-TCA GGC ACA TGC ATG TCT GT-3'	5'-CCA AGG AGT CTG CTT CT CTT-3'
RT-PCR		
<i>lncRNA-HSVIII</i>	5'-CAC CTG TTC CTT GAC TTG AT-3'	5'-GTG TGT ATT CAG GTA TGT GC -3'
<i>Gapdh</i>	5'-CAT GAC CAC AGT CCA TGC CAT C -3'	5'-TAG CCC AAG ATG CCC TTC AGT G-3'
<i>Gapdh</i> (in5-ex6)	5'-CCT TCT TTG TAG GTG TCC CT-3'	5'-TAG CCC AAG ATG CCC TTC AGT G-3'
<i>Gapdh</i> (ex5-ex6)	5'-TTG TGA TGG GTG TGA ACC AC -3'	5'-TAG CCC AAG ATG CCC TTC AGT G-3'
5'RACE and 3'RACE		
Abridged Anchor Primer	5'-GGC CAC GCG TCG ACT AGT ACG GGI IGG GII GGG IIG-3'	
Abridged Universal Amplification Primer	5'-GGC CAC GCG TCG ACT AGT AC-3'	
3 sites Adaptor Primer		5'-CTG ATC TAG AGG TAC CGG ATC C-3'
RT-1		5'-TGC AGC TTG AAA AAT GTG AA-3'
GSP1		5'-CAC TAC CGA ATC ACA AGA TC-3'
GSP2		5'-ATC AAG TCA AGG AAC AGG TG-3'
GSP3	5'-AGT ATA GAG GAG CTC TTA TC-3'	
GSP4	5'-GTG CAT GAG GGC CTT AGT TT-3'	
Chromosome conformation capture assay		
anchor primer	5'-CAT AAG GCG TAG AAA ATA CG-3'	
HSI		5'-TGG AGA GAG GGA AAG AAG GA-3'
HSIV		5'-TTG TCT TTA GTA TGG AGT GT-3'
<i>Tessp-2</i> promoter		5'-CCT CCA TCT CCC AGT AAG GT-3'
<i>Tessp-3</i> promoter		5'-TCC TCC TTC TGT CCC TCA GA-3'
<i>Tessp-4</i> promoter		5'-CCA CTG CCT GGC AAG AAT TT-3'
<i>Tessp-4</i> 3' region		5'-CCA GGA GGT TGT GTA GCA AA-3'
<i>Tessp-3</i> and <i>Tessp-4</i> intergenic region		5'-GGC TTC TCA AGA TTA TAG TG-3'
<i>Ercc3</i> forward-1	5'-CTC TTC CTG GGT CTG TCG AT-3'	
<i>Ercc3</i> forward-2	5'-TGA GAT CGT CAC ACG TCC TT-3'	
Plasmid Constructs		
<i>Tessp-2</i> promoter	5'-CCA AGT ACA CTG TAG CTG TC-3'	5'-GTC ATC ACG TAG GCC ACC CT-3'
5' half of <i>lncRNA-HSVIII</i>	5'-TTC ATC TTC CCT CAC TAG TCA TCA TTT G-3'	5'-ACC AGG CTG GCT TCG AAC TTA C-3'
3' half of <i>lncRNA-HSVIII</i>	5'-AGT ATA GAG GAG CTC TTA TC-3'	5'-TTT TCT TTT CTT TTC TTT TCT TTT CTT TTC TTT TCT CTG TGT-3'

Figure 1

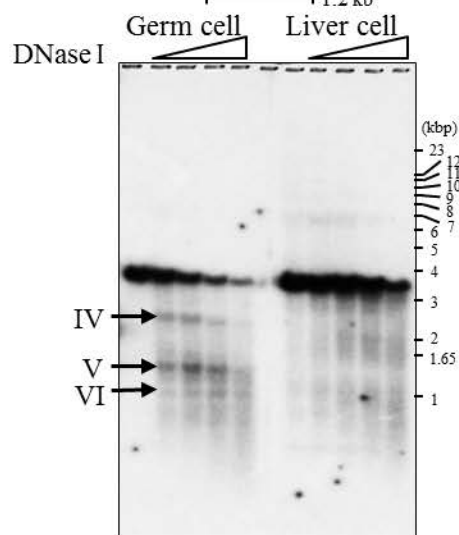
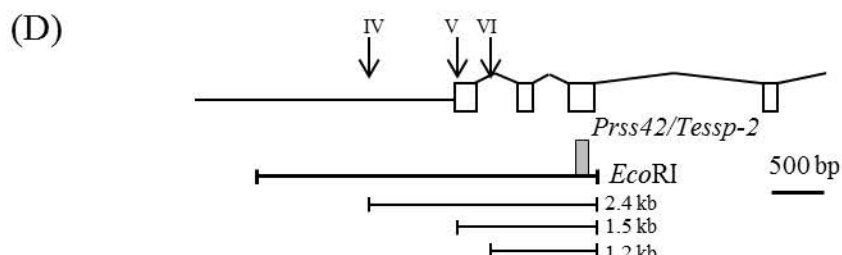
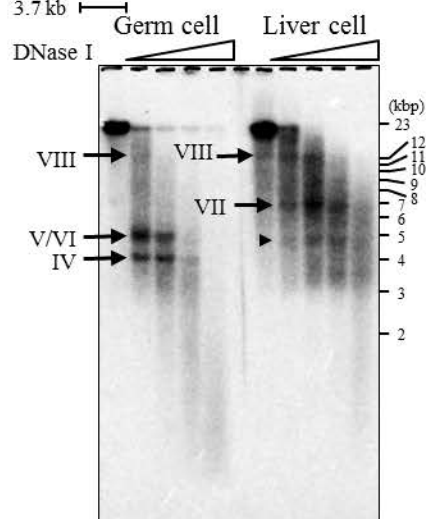
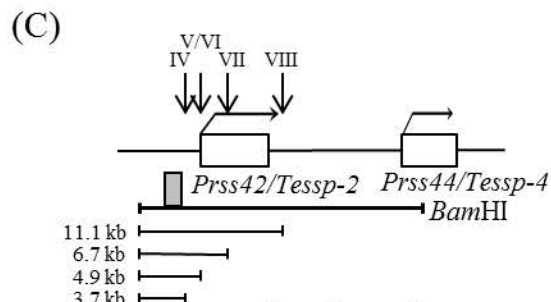
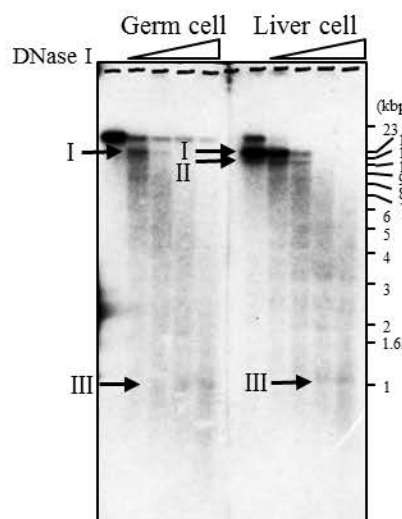
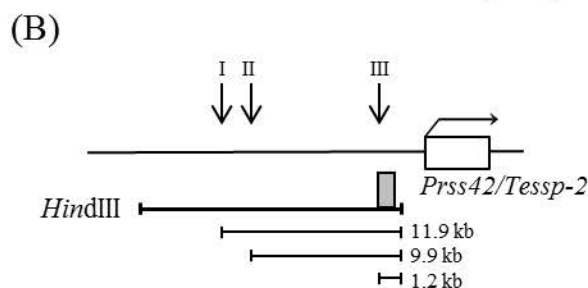
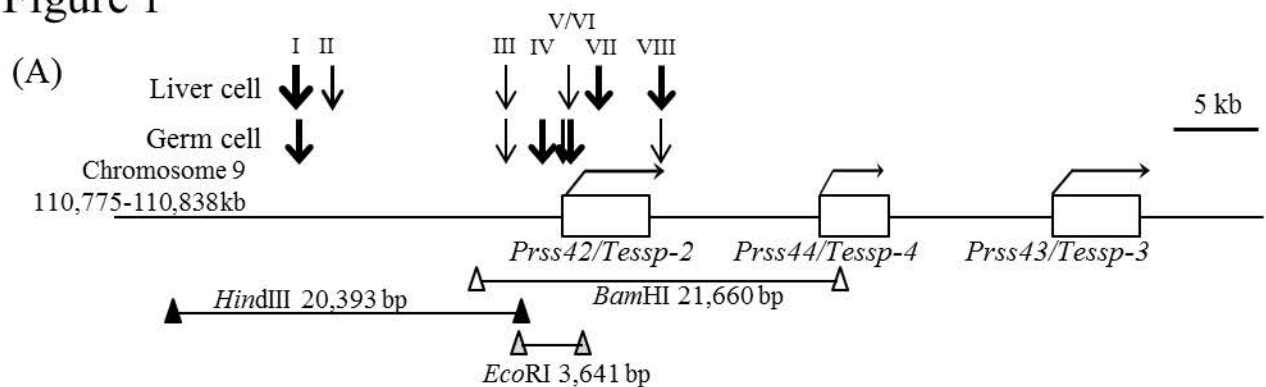


Figure 2

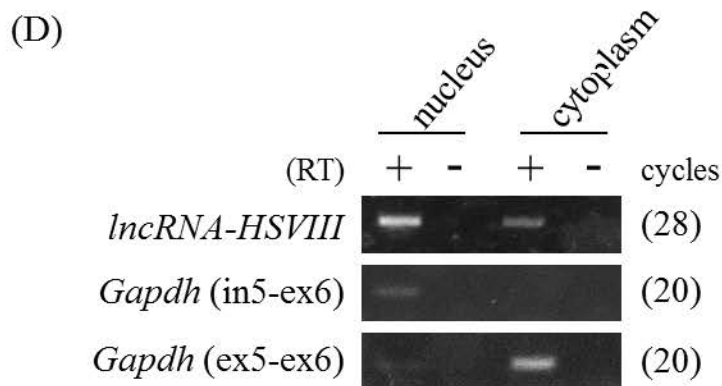
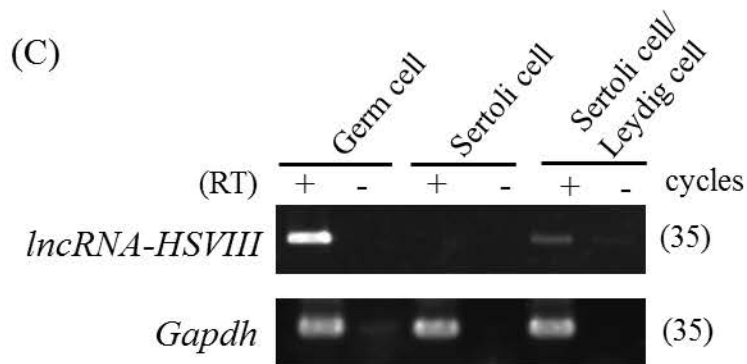
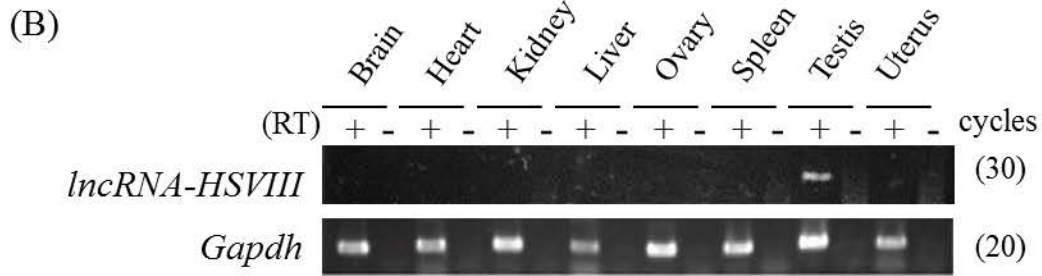
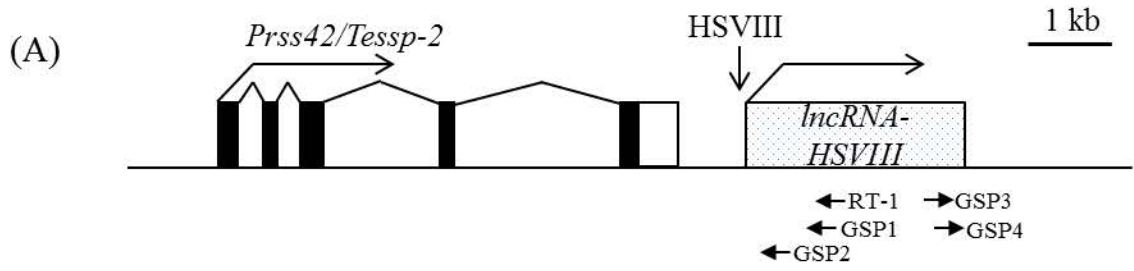


Figure 3

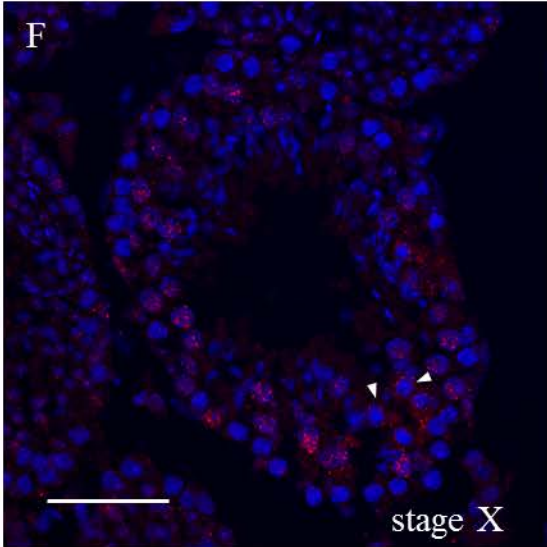
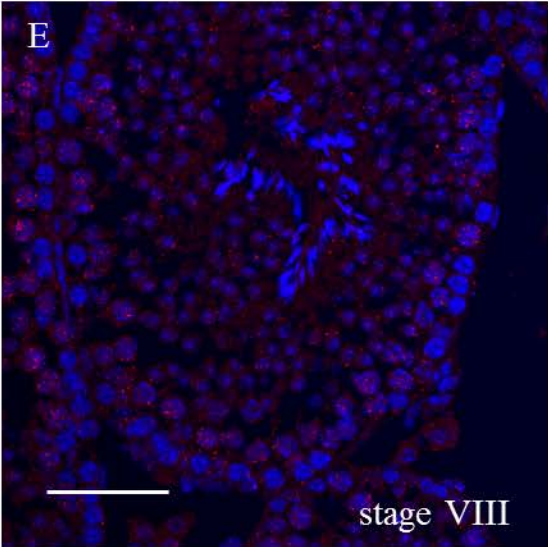
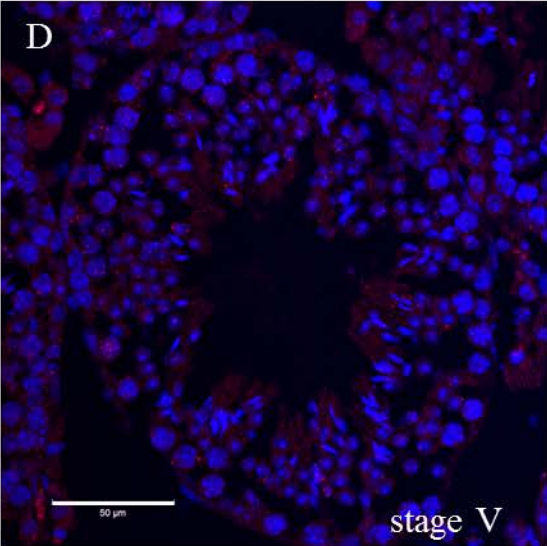
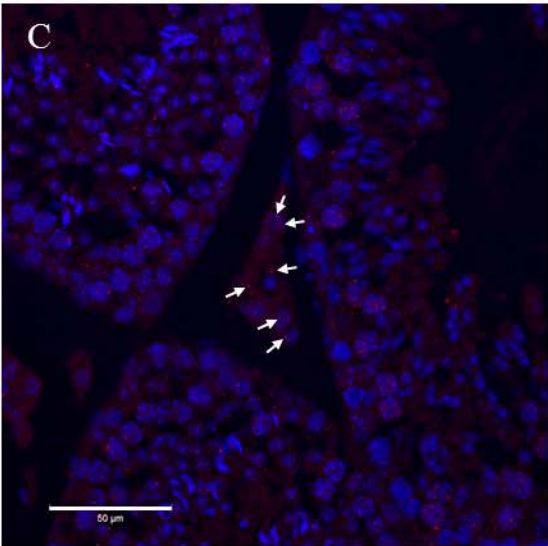
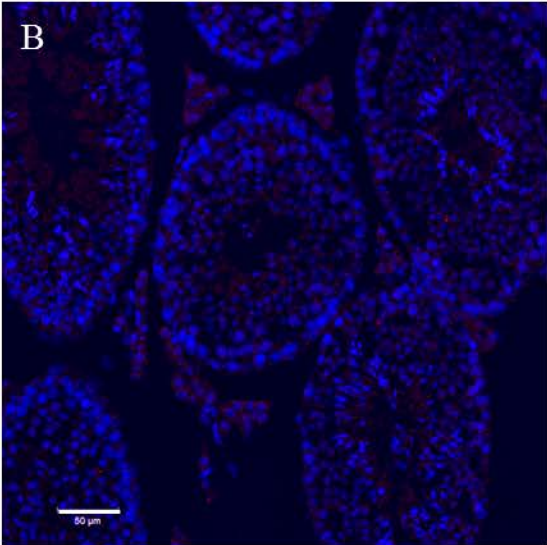
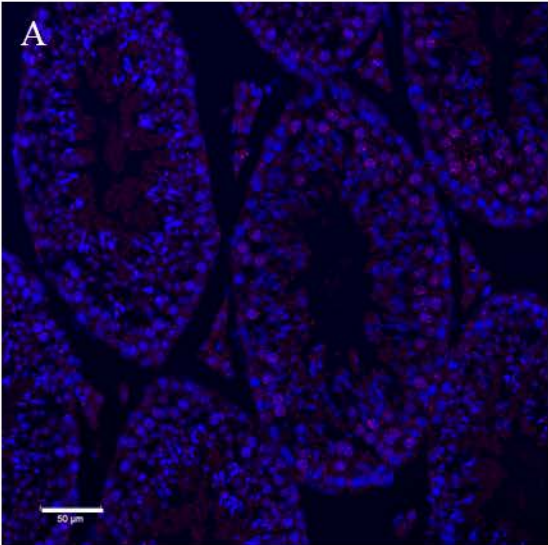
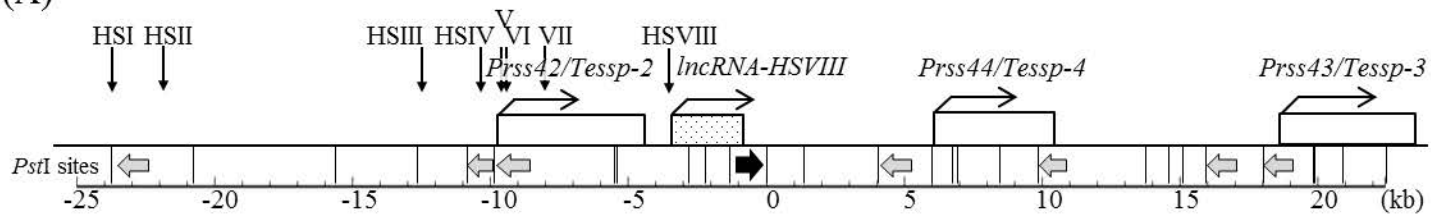
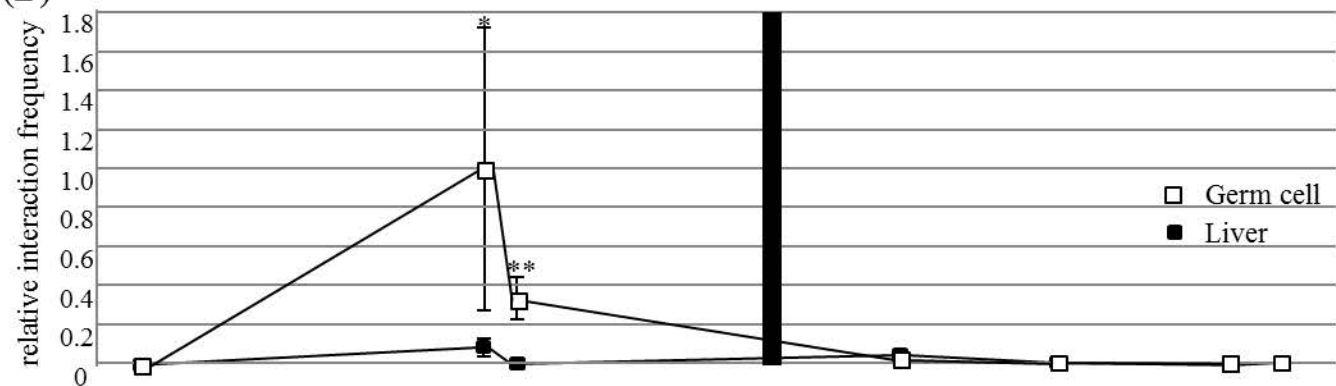


Figure 4

(A)



(B)



(C)

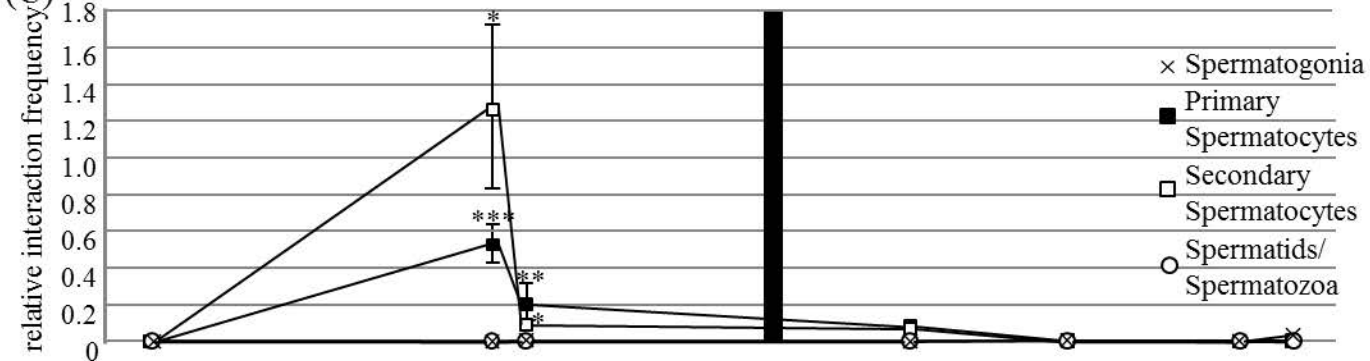
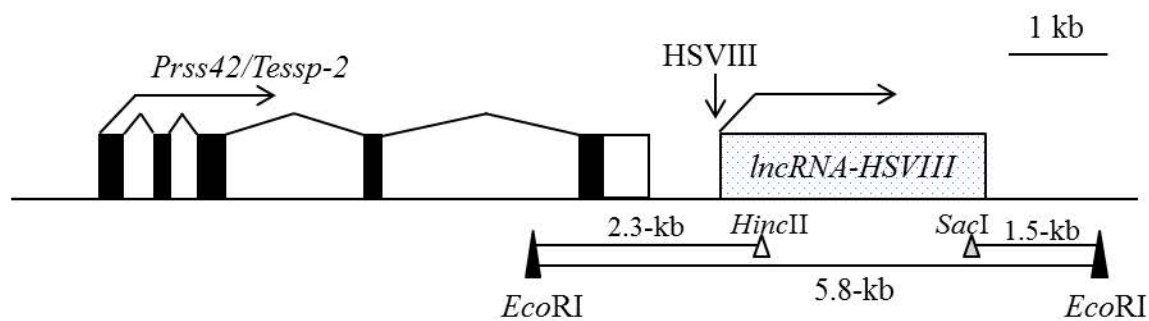
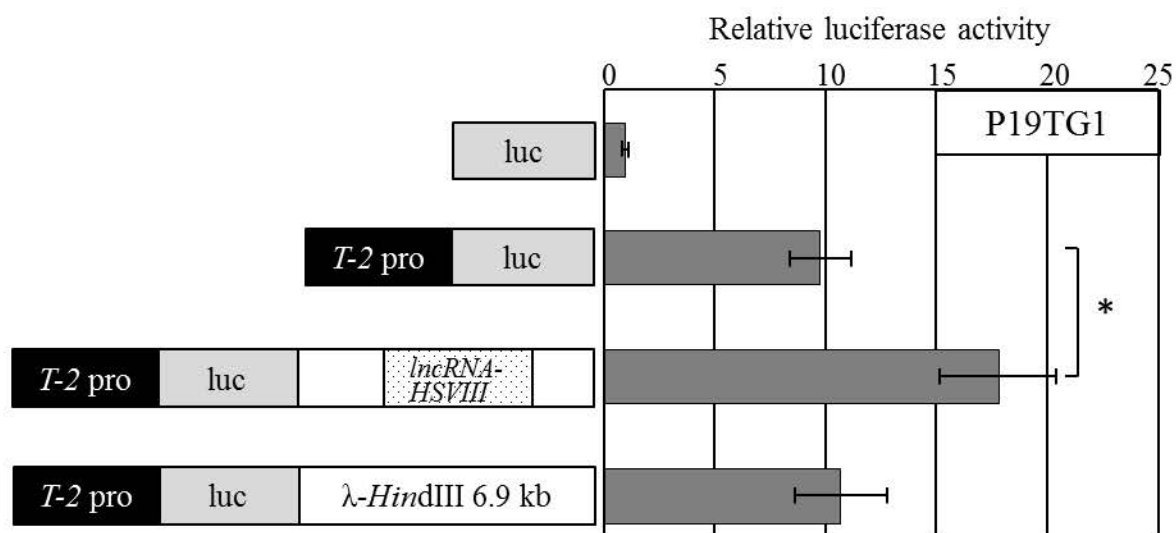


Figure 5

(A)



(B)



(C)

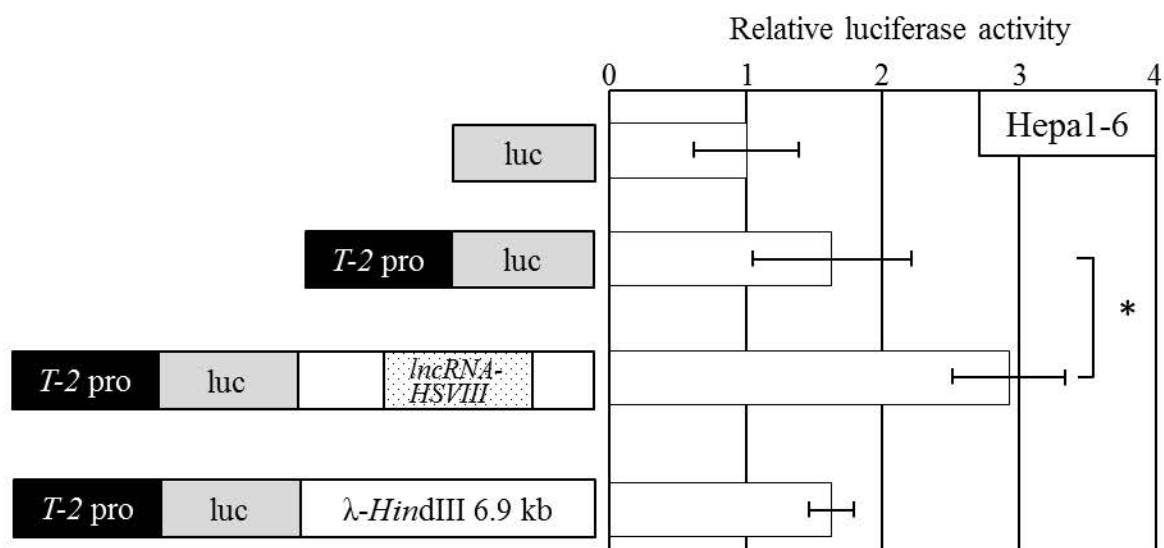


Figure 6

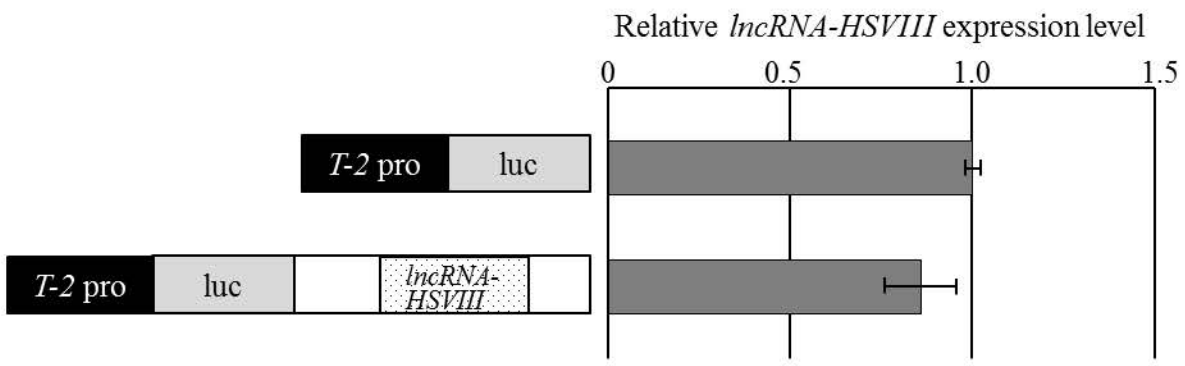


Figure 7

